Mathematical model of adult stem cell regeneration with cross-talk between genetic and epigenetic regulation

Jinzhi Lei[a], Simon A. Levin[b,1], and Qing Nie[c]

[a]Zhou Pei-Yuan Center for Applied Mathematics, Ministry of Education Key Laboratory of Bioinformatics, Tsinghua University, Beijing 100084, China; [b]Department of Ecology and Evolutionary Biology, Princeton University, Princeton, NJ 08544; and [c]Department of Mathematics, University of California, Irvine, CA 92697

Contributed by Simon A. Levin, January 7, 2014 (sent for review September 4, 2013)

Adult stem cells, which exist throughout the body, multiply by cell division to replenish dying cells or to promote regeneration to repair damaged tissues. To perform these functions during the lifetime of organs or tissues, stem cells need to maintain their populations in a faithful distribution of their epigenetic states, which are susceptible to stochastic fluctuations during each cell division, unexpected injury, and potential genetic mutations that occur during many cell divisions. However, it remains unclear how the three processes of differentiation, proliferation, and apoptosis in regulating stem cells collectively manage these challenging tasks. Here, without considering molecular details, we propose a genetic optimal control model for adult stem cell regeneration that includes the three fundamental processes, along with cell division and adaptation based on differential fitnesses of phenotypes. In the model, stem cells with a distribution of epigenetic states are required to maximize expected performance after each cell division. We show that heterogeneous proliferation that depends on the epigenetic states of stem cells can improve the maintenance of stem cell distributions to create balanced populations. A control strategy during each cell division leads to a feedback mechanism involving heterogeneous proliferation that can accelerate regeneration with less fluctuation in the stem cell population. When mutation is allowed, apoptosis evolves to maximize the performance during homeostasis after multiple cell divisions. The overall results highlight the importance of cross-talk between genetic and epigenetic regulation and the performance objectives during homeostasis in shaping a desirable heterogeneous distribution of stem cells in epigenetic states.

fitness function | optimization | robustness | dynamic programming | systems biology

Adult stem cells are present in most self-renewing tissues, including skin, intestinal epithelium, and hematopoietic systems. Stem cells provide regeneration through proliferation, differentiation, and apoptosis; therefore, the accumulation of undesirable epigenetic changes, which are independent of the genetic instructions but heritable at each cell division, can lead to the causation or progression of diseases (1, 2). Epigenetic effects such as the stochastic partitioning of the distribution of regulatory molecules during cell division may change the capability of the cell to undergo differentiation or proliferation (3), and the accumulation of DNA errors (or damages) can result in carcinogenesis (4–6).

Many stem cells are heterogeneous in their ability to proliferate, self-renew, and differentiate, and they can reversibly switch between different subtypes under stress conditions. Specifically, hematopoietic stem cells (HSCs) (see ref. 7 for a review of HSC heterogeneity) have distinguished subtypes (such as lymphoid deficient, balanced, or myeloid deficient) whose distribution depends on their heterogeneity during the differentiation process (7, 8). HSCs can reversibly acquire at least three proliferative states: a dormant state in which the cells are maintained in the quiescent stage of the cell cycle, a homeostatic state in which the cells are occasionally cycling, and an injury-activated state in which the cells are continuously cycling (9, 10). Each state is likely associated with a unique microenvironment (10, 11). Dormant and homeostatic HSCs are anchored in endosteal niches through interactions with a number of adhesion molecules expressed by both HSCs and niche stromal cells (10, 12). Furthermore, injury-activated HSCs are located near sinusoidal vessels (the perivascular niche). In response to the loss of hematopoietic cells, surviving dormant HSCs located in their niches develop into injury-activated HSCs to undergo self-renewing divisions. In the recovery stage, injury-activated HSCs either differentiate into multipotential progenitor cells or migrate to their osteoblastic niches to reestablish the dormant and homeostatic HSC pools (10, 13).

The growth and regeneration of many adult stem cell pools are tightly controlled with feedback regulation at different levels. For example, HSC self-renewal and differentiation are regulated by direct HSC–niche interactions and cytokines secreted from stromal cells through various feedback signals (9–11). Adult intestinal stem cells residing in a niche in the crypt are regulated by the paracrine secretion of growth factors and cytokines from surrounding mesenchymal cells (14–16). In addition, the mammalian olfactory epithelium, a self-renewing neural tissue, is regulated through negative feedback signals involving the diffusive molecules GDF11 and activin (17).

Independent of division modes, symmetric or asymmetric cell divisions may lead to daughter cells with genetic or epigenetic states different from the normal states. The enormous functional demands and longevity of stem cells suggest that stem cells, par-

Significance

This paper examines how adult stem cells maintain their ability to carry out a complex set of tasks, including tissue regeneration and replacement of defective cells. To do so, stem cell populations must coordinate differentiation, proliferation, and cell death (apoptosis) to maintain an appropriate distribution of epigenetic states. Using the tools of applied mathematics, and borrowing from the theory of intergenerational transfer of resources, this paper shows how control strategies during cell division should be chosen to maximize expected performance, utilizing cross-talk between genetic and epigenetic regulation and performance criteria during homeostasis. Heterogeneous proliferation, a mixed strategy in which not all cells have the same proliferation probability, is shown to increase robustness, and hence long-term performance.

Author contributions: J.L., S.A.L., and Q.N. designed research; J.L. and Q.N. performed research; J.L., S.A.L., and Q.N. contributed new reagents/analytic tools; J.L. and Q.N. analyzed data; and J.L., S.A.L., and Q.N. wrote the paper.

The authors declare no conflict of interest.

See Commentary on page 3653.

[1]To whom correspondence should be addressed. E-mail: slevin@princeton.edu.

This article contains supporting information online at www.pnas.org/lookup/suppl/doi:10.1073/pnas.1324267111/-/DCSupplemental.

ticularly the cells from highly regenerative tissues (e.g., epithelium or blood), may be equipped with effective repair mechanisms to ensure genomic integrity over a lifetime (18). Stem cells often respond differently to genetic or epigenetic errors at different proliferation phases (19). Studies regarding the population response to DNA damage of HSCs have suggested that the system selects for the least damaged cells, and the competition between different cells is controlled by the level of p53 proteins (20, 21). Highly regenerative adult stem cells (e.g., HSCs) need to possess effective strategies that balance long-term regeneration with protection from mutagenesis (for example, cell proliferation or differentiation may be affected by the DNA damage response) (20, 22).

Previous modeling studies based on the cell population dynamics have indicated that feedback regulation to the proliferation is important to maintain the homeostasis of tissue growth (23–25). The exploration and analysis of models that include transit-amplifying progenitor cells and terminally differentiated cells have suggested that multiple feedback mechanisms at different lineage stages can influence the speed of tissue regeneration for better performance (17, 26–28). These population dynamic models could include age structure (29), evolution (27, 30), and stochasticity (30, 31); and these models could also be applied to the regulation of cancer (32). Studies based on spatial modeling have found that diffusive and regulatory molecules involved in feedback mechanisms regulating the differentiation capabilities of the cells are important in maintaining the stem cell niche and shaping tissue stratification (33, 34).

During the tissue self-renewal process driven by adult stem cells, how do stem cells maintain a desirable distribution of epigenetic states over their lifetimes despite many perturbations or accidental changes? What are the controlling strategies that enable a cell to maximize its performance at each cell cycle while contributing positively to the entire cell population during tissue growth? Additionally, are these control strategies able to guide genetic evolution to achieve high tissue performance over a long period? Without considering any molecular details, we present a dynamic programming model that includes stochastic transitions between cell cycles. The model is defined by the combination of a performance function at each cell division and a fitness function during tissue homeostasis. We sought optimal controlling strategies involving proliferation, differentiation and apoptosis that naturally and collectively emerge from achieving performance objectives as well as optimizing fitness. The model, which represents stem cells as a distribution of a state variable, emphasizes the cross-talk between genetic evolution and epigenetic states and their stochastic transitions at each cell cycle. The analysis and computation of the model suggest the existence of several critical controlling strategies that regulate proliferation and apoptosis and are highlighted by heterogeneous dependence on the epigenetic states in the feedback regulation.

Results

A Model of Stem-Cell Regeneration with Epigenetic Transition. The model is based on the G_0 cell cycle model (35, 36) and a dynamic programming approach for intergenerational resource transfer (37, 38) together with evolutionary dynamics (39). Stem cells at cell cycling are classified into resting (G_0) or proliferating (G_1, S, and G_2 phases and mitosis) phases (Fig. 1*A*) (35). During each cell cycle, a cell in the proliferating phase either undergoes apoptosis or divides into two daughter cells; however, a cell in the resting phase either irreversibly differentiates into a terminally differentiated cell or returns to the proliferating phase. In some tissues, resting phase cells (e.g., HSCs) may undergo a reversible transition to a quiescent phase with preserved self-renewal, which results in two distinct cell populations.

To study the heterogeneity of cell responses, we denote x as the epigenetic state of a cell, which, for example, can be the expression levels of one or multiple genes, the number of nucleosome modifications of a DNA region, or the positions of DNA methylation. In short, x represents one or several

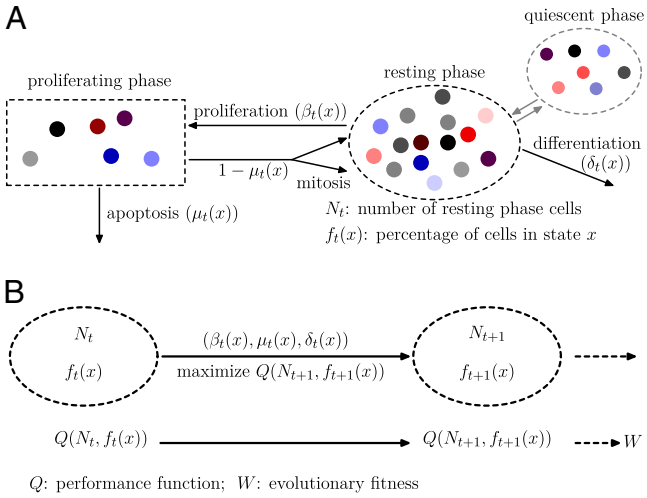

Fig. 1. Model Illustration. (*A*) At the *t*th cell cycle, cells in the resting phase either enter the proliferating phase with the probability of β_t, or differentiate into other cell types with the probability of δ_t. The proliferating cells undergo apoptosis with the probability of μ_t. Resting phase cells occasionally migrate to the quiescent phase and vice versa under stress. (*B*) The performance function $Q(N_t,f_t(x))$ quantifies how well the tissue fits to its physiological properties. The changes in the tissue state $(N_t,f_t(x))$ at each cell cycle are determined by the three quantities $\{\beta_t(x),\mu_t(x),\delta_t(x)\}$ chosen to maximize the performance at the next cycle to give $Q(N_{t+1},f_{t+1}(x))$. An evolutionary fitness function at homeostasis, denoted by W, is the limit of $Q(N_t,f_t(x))$ when $t\to\infty$.

intrinsic cellular states that may change during cell division. Here, only epigenetic states that are significant for cell differentiation, proliferation, or apoptosis are considered. Consequently, the three processes have dependences on the epigenetic state x: $\delta_t(x)$, $\beta_t(x)$, and $\mu_t(x)$, where the subscript t indicates the tth cell cycle (Fig. 1).

The distribution density of stem cells during the resting phase, whose total population is denoted as N_t, with different epigenetic states x, is characterized by $f_t(x)$. $(N_t,f_t(x))$ undergoes a transformation from one cell cycle to the next (Fig. 1*B*):

$$(N_t,f_t(x))\mapsto(N_{t+1},f_{t+1}(x)). \qquad [1]$$

During each cell cycle, $N_t\int f_t(x)\delta_t(x)dx$ cells leave the resting phase due to differentiation, and $N_t\int f_t(x)\beta_t(x)dx$ cells enter the proliferating phase. Each cell in the proliferating phase either undergoes apoptosis with a probability of $\mu_t(x)$ or produces two daughter cells. Hence, the cell population after mitosis is

$$\begin{aligned} N_{t+1} &= N_t - N_t\int f_t(x)\delta_t(x)dx - N_t\int f_t(x)\beta_t(x)dx \\ &\quad + 2N_t\int f_t(x)\beta_t(x)(1-\mu_t(x))dx \\ &= N_t\left(1+\int f_t(x)[\beta_t(x)(1-2\mu_t(x))-\delta_t(x)]dx\right). \end{aligned}$$

The integrals are taken over all possible epigenetic states. In this derivation, the reversible transition between the resting phase and the quiescent phase is regarded as perfectly balanced for an equilibrium, which may occur during homeostasis. In this paper, we only considered the effect of this transition for regeneration in response to a severe loss of differentiated cells (*SI Text*, section S3).

We define the observed proliferation probability as

$$\beta_{t,\mathrm{obs}} = 1+\int f_t(x)[\beta_t(x)(1-2\mu_t(x))-\delta_t(x)]dx, \qquad [2]$$

then

$$N_{t+1} = N_t \beta_{t,\text{obs}}. \quad [3]$$

Here $\beta_{t,\text{obs}}$ is the ratio of the cell population numbers between two consecutive cell cycles.

To account for stochastic effects during the inheritance of epigenetic states that lead to variability of daughter cells in each cell division (3, 40, 41), we introduced an inheritance probability $p(x,y)$, which represents the probability that a daughter cell of state x comes from a mother cell of state y. Therefore, $\int p(x,y)dx = 1$ for any y. Similarly to the above argument, we obtained (*SI Text*, section S1)

$$f_{t+1}(x) = \frac{1}{\beta_{t,\text{obs}}}\left[f_t(x)(1-(\delta_t(x)+\beta_t(x))) + 2\int f_t(y)\beta_t(y)(1-\mu_t(y))p(x,y)dy\right]. \quad [4]$$

Eqs. **3** and **4** define a transformation between two cell cycles.

During the tissue homeostasis, Eq. **3** indicates that the observed proliferation satisfies $\beta_{t,\text{obs}} \to 1$ as $t \to \infty$. Otherwise, either uncontrolled growth ($\beta_{t,\text{obs}} > 1$) or tissue degeneration ($\beta_{t,\text{obs}} < 1$) occurs. Hence, cell proliferation, differentiation, and apoptosis (i.e., $\{\beta_t(x), \mu_t(x), \delta_t(x)\}$) must be dynamically controlled at each cell cycle, for example, through signal molecules released from downstream cell lineages (17, 32). This dynamic regulation leads to a limited distribution at homeostasis,

$$f(x) = \lim_{t\to\infty} f_t(x), \quad [5]$$

which describes the stem cell distribution as a function of epigenetic states, and is termed "tissue epigenetics" for short.

One possible control strategy for this type of growth may follow evolution akin to natural selection (42). To model this selection, we first introduced a tissue performance function Q depending on the population of stem cells through a function φ as well as the distribution of epigenetic states x in the tissue through a cell performance function $\chi(x)$, so that the performance at the tth cell cycle is given by

$$Q(N_t, f_t(x)) = \varphi(N_t)\int \chi(x) f_t(x)dx. \quad [6]$$

The cell performance $\chi(x)$ measures the capability of a cell with given epigenetic state x in accomplishing its physiological functions (see Fig. 2 as an example). A larger value corresponds to better performance.

We assumed that two layers of regulation occur between two cell cycles: one at the epigenetic level that occurs at each cell division, and one at the genetic level that is selected by mutations over a long time scale of many cell divisions. In particular, the probability of proliferation $\beta_t(x)$ varies at each cell cycle by epigenetic regulation, while the apoptosis probability $\mu_t(x) = \overline{\mu}_G(x) + \hat{\mu}_t(x)$, in which $\overline{\mu}_G(x)$ is the average probability at homeostasis and is selected through genetic mutations over a long time scale and $\hat{\mu}_t(x)$ is random at each cell cycle due to epigenetic modulations. Similarly, the differentiation probability takes the form of $\delta_t(x) = \overline{\delta}_G(x) + \hat{\delta}_t(x)$ in which $\overline{\delta}_G(x)$ is the average probability at homeostasis and $\hat{\delta}_t(x)$ represents epigenetic uncertainty. With these mechanisms of regulation, the performance Q after cell division depends, through Eqs. **2–4**, on the proliferation $\beta_t(x)$ as well as the stochasticities in apoptosis $\mu_t(x)$ and differentiation $\delta_t(x)$. Thus, we can write the performance function after cell division as (*SI Text*, section S1)

$$Q(N_{t+1}, f_{t+1}(x)) = Q(N_t, f_t(x)|\beta_t(x), \mu_t(x), \delta_t(x)). \quad [7]$$

During each cell cycle, the proliferation $\beta_t(x)$ is controlled to achieve maximum tissue performance after cell division in the face of uncertainties in apoptosis $\mu_t(x)$ and differentiation $\delta_t(x)$, which leads to solving the corresponding Bellman condition (38, 43–45)

$$\mathrm{E}_{\mu_t(x),\delta_t(x)} \max_{\beta_t(x)} Q(N_t, f_t(x)|\beta_t(x), \mu_t(x), \delta_t(x)), \quad [8]$$

where $\mathrm{E}_{\mu_t(x),\delta_t(x)}$ is the expectation with respect to apoptosis and differentiation probabilities during cell division.

The evolutionary fitness function is defined as the performance at homeostasis after multiple cell divisions (i.e., $t \to \infty$; see also Fig. 1*B*):

$$W = \lim_{t\to\infty} Q(N_t, f_t(x)). \quad [9]$$

While the tissue performance function Q is subject to epigenetic regulation at each cell cycle, the fitness function W is genetically regulated and dependent on the apoptosis $\overline{\mu}_G(x)$ and the differentiation $\overline{\delta}_G(x)$. Evolution selects $\overline{\mu}_G(x)$ and $\overline{\delta}_G(x)$ through mutations to maximize the fitness W. The overall model defines a principle of a control strategy that incorporates cross-talk between genetic and epigenetic regulation in stem cell regeneration and evolution.

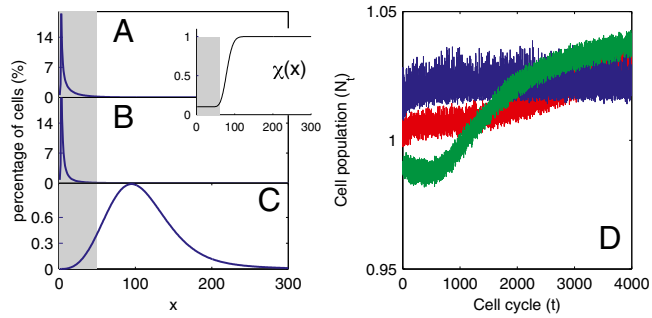

Fig. 2. Distribution of cells at homeostasis under three different combinations of the epigenetic regulation. (*A*) Both $\beta(x)$ and $\overline{\mu}_G(x)$ are independent of x, and $\overline{\delta}_G(x)$ changes with x. (*Inset*) The performance function $\chi(x)$ is shown. (*B*) $\overline{\mu}_G(x)$ is independent of x, and $\beta(x)$ and $\overline{\delta}_G(x)$ change with x. (*C*) Both $\overline{\delta}_G(x)$ and $\beta(x)$ are independent of x, and $\overline{\mu}_G(x)$ changes with x. Shadow regions ($x < 60$) represent defective states. (*D*) Time course of N_t under the three conditions (red, green, and blue for conditions A–C, respectively). (See *SI Text*, section S5 for details on simulations.)

Heterogeneous Apoptosis Can Improve the Maintenance of Tissue Epigenetics. During growth, the accumulation of stochastic modifications in epigenetic states may produce defective cells that need to be effectively repaired or removed. Here, we show that heterogeneous apoptosis is advantageous in controlling tissue epigenetics.

First, the epigenetic function $f(x)$, when we take $t \to \infty$ in Eqs. **3** and **4** with an assumption of no epigenetic uncertainty in differentiation and apoptosis, satisfies the following integral equation (*SI Text*, section S2):

$$f(x) = \frac{2\int f(y)\beta(y)(1-\overline{\mu}_G(y))p(x,y)dy}{\overline{\delta}_G(x)+\beta(x)}, \quad [10]$$

where $\beta(x) = \lim_{t\to\infty}\beta_t(x)$ satisfies

$$\int f(x)\left[\beta(x)(1-2\overline{\mu}_G(x)) - \overline{\delta}_G(x)\right]dx = 0. \quad [11]$$

Analysis of a simplified model based on Eqs. **10** and **11** shows that homogenous apoptosis [i.e., $\overline{\mu}_G(x)$ is independent of x] easily leads to abnormal or disease conditions for a tissue (*SI Text*,

section S2). This observation is further confirmed by direct simulations of Eqs. **10** and **11** under the condition in which apoptosis probability $\overline{\mu}_G(x)$ is either dependent on or independent of x (Fig. 2). Whenever the apoptosis $\overline{\mu}_G(x)$ is independent of x, most cells accumulate in low-performance states (Fig. 2 *A* and *B*). In contrast, if $\overline{\mu}_G(x)$ is dependent on x so that the cells with lower performance have a greater probability of apoptosis, only a small number of low-performance cells are present during homeostasis (Fig. 2*C*). These results suggest that heterogeneity in apoptosis can improve the maintenance of acceptable tissue epigenetics during a long lifespan.

Furthermore, we find that heterogeneity in the cell performance function ($\chi(x)$) is important for successful natural selection of apoptosis strategies, and epigenetic transition during cell division is helpful for robust tissue epigenetics during homeostasis with respect to accidental changes in the tissue lifespan (*SI Text*, section S3). Interestingly, despite apparent differences in tissue epigenetics, homogeneous or heterogeneous apoptosis yields similar dynamics in the cell population N_t (Fig. 2*D*), demonstrating the importance of introducing the function $f_t(x)$ for epigenetic states into the model. The cell population model alone may be insufficient to study the control strategies of stem cell regeneration.

An Optimal Control for Proliferation During Each Cell Cycle Depends on Complex Feedback Regulation Involving the Epigenetic States and the Size of the Total Cell Population. Optimal control at each cell cycle involves identifying the proliferation probability to maximize the performance Q in Eq. **8** after cell division. To study the system analytically, we considered two cases based on either homogeneous or heterogeneous proliferation.

Homogeneous proliferation (strategy A). When $\beta_t(x)$ is independent of the epigenetic state x, meaning that all cells in the tissue are alike in their ability to undergo cell cycle reentry, the optimal proliferation (strategy A) is governed by $\partial Q/\partial\beta_t = 0$, which yields

$$\frac{N_t\beta_{t,\mathrm{obs}}\varphi'\left(N_t\beta_{t,\mathrm{obs}}\right)}{\varphi\left(N_t\beta_{t,\mathrm{obs}}\right)} = A_t, \qquad [12]$$

where A_t is a quantity determined by $f_t(x), \delta_{t-1}(x), \mu_{t-1}(x)$ (*SI Text*, section S3). The proliferation β_t is obtained from Eq. **12** by solving $\beta_{t,\mathrm{obs}}$. In particular, when N_t is near the value N_* that maximizes the function φ, β_t can be approximated by

$$\beta_t \approx \frac{\frac{1}{N_t}\left(N_* + \frac{A_t\varphi(N_*)}{N_*\varphi''(N_*)}\right) - 1 + \overline{\delta}_t}{1 - 2\overline{\mu}_t}. \qquad [13]$$

Here $\overline{\delta}_t$ and $\overline{\mu}_t$ are average probabilities of differentiation and apoptosis, respectively. Examples of tissue dynamics based on strategy A are shown in *SI Text*, section S3.

A direct consequence of Eq. **13** is that the proliferation β_t decreases with the cell population, resulting in a negative feedback control. We note that the tissue epigenetics in the next cell generation $f_{t+1}(x)$ depends on the current generation proliferation β_t through Eq. **4**, leading to complex negative feedback regulation during each cell cycle.

Heterogeneous proliferation (strategy B). Next, we considered the case of cells having two distinct proliferation probabilities. In these two distinct states, denoted by $x \in \Omega_1$ or $x \in \Omega_2$, we assumed

$$\beta_t(x) = \begin{cases} \beta_{t,1}, & x \in \Omega_1 \\ \beta_{t,2}, & x \in \Omega_2. \end{cases} \qquad [14]$$

In addition, we assumed that type I cells, defined as cells with $x \in \Omega_1$, are unmodulated at each cell cycle (i.e., $\beta_{t,1} \equiv \overline{\beta}_{1,G}$ is genetically regulated), and type II cells, defined as cells with $x \in \Omega_2$, are modulated such that $\beta_{t,2}$ changes at each cell cycle. Biologically, this assumption corresponds to the situation in which, for example, certain growth factor receptors are active (or expressed) only in type II but not type I cells; however, the receptors are required to respond to external signals to control proliferation.

The probability $\beta_{t,2}$ (strategy B) is determined by $\partial Q/\partial\beta_{t,2} = 0$, which yields an equation for $\beta_{t,\mathrm{obs}}$ similar to Eq. **12**. In particular, when N is close to the value N_* (*SI Text*, section S3), one has

$$\beta_{t,2} \approx \frac{\frac{1}{N_t}\left(N_* + \frac{A_t'\varphi(N_*)}{N_*\varphi''(N_*)}\right) - 1 - \overline{\beta}_{1,G}\left(\overline{f}_{t,1} - 2\overline{\mu}_{t,1}\right) + \overline{\delta}_t}{\overline{f}_{t,2} - 2\overline{\mu}_{t,2}}. \qquad [15]$$

All bar terms are averages over cell epigenetic states, with a subscript 1 for type I cells ($x \in \Omega_1$) and a subscript 2 for type II ($x \in \Omega_2$). Similarly to $\overline{\delta}_t$ and $\overline{\mu}_t$ in Eq. **13**, these average terms incorporate genetic and epigenetic regulation in differentiation and apoptosis. Examples of tissue dynamics based on strategy B are shown in *SI Text*, section S3.

Eq. **15** shows that $\beta_{t,2}$ is a decreasing function of the cell population, resulting in a complex negative feedback regulation with respect to cell populations and the epigenetic states of the tissue cells. We note that the heterogeneous proliferation probability $\beta_{t,2}$ for the type II cells also depends on the probability of the type I cells, which suggests that an appropriate selection of the unmodulated proliferation $\overline{\beta}_{1,G}$ can improve the performance at homeostasis in comparison with homogenous cells (*SI Text*, section S3).

Simple feedback via the size of the cell population (strategy C). Optimal controls of proliferation based on our model lead to the negative feedback regulation of proliferation through the cell population. Similar regulatory mechanisms with negative feedback have been explicitly introduced in many stem cell population models (17, 27, 36, 46) by use of a Hill function (strategy C) such as

$$\beta_t = \beta_0\frac{1 + \rho(N_t/K)^m}{1 + (N_t/K)^m}, \qquad [16]$$

where β_0, ρ, K, m are constants.

A major difference between Eqs. **16** and **13** or **15** based on our model is that the coefficients in Eq. **16** are constants and independent of the tissue epigenetics. Thus, strategy C is a simple feedback mechanism involving only the cell population; however, both strategies A and B are complex feedback mechanisms incorporating both cell population and tissue epigenetics. The importance of epigenetic states has recently been implicated during the stem cell self-renewal and differentiation processes (47, 48). This epigenetic dependence of feedback mechanisms, as shown in the next section, can improve the robustness in tissue dynamics.

Heterogeneous Proliferation Is Important for the Robustness of Growth with Respect to Sudden Changes. During the lifespan of an organism, many unexpected alterations to stem cell systems occur at various levels, such as the loss of stem cells (e.g., injury or marrow donation) and temporal changes in cell differentiation and apoptosis capabilities (several studies have reported a 20-fold increase in the differentiation activity of HSCs under the administration of G-CSF) (49). In many situations, stem cell tissues recover in a timely manner after these types of changes. For example, most marrow donors complete recovery within a few weeks (50, 51) (see also http://bethematch.org), corresponding to ~10 cell cycles of HSCs (each cell cycle is approximately 1.4 – 4.2 d according to ref. 24). Many donors even recover in less than 5 d (51). Therefore, a physiologically reliable control strategy should induce fast adaptation and robust recovery against these changes.

Here, we studied the three different strategies (A, B, and C) in response to changes in the stem cell population. Two types of changes were studied: a sudden decrease in the cell population

and a temporary increase in the differentiation probability. First, we examined the recovery dynamics after a sudden loss of the cell population to approximately half of the normal level (all cell types were equally lost). Both strategies A and B induced fast recovery of the cell populations in ~10 cell cycles (Fig. 3). However, using strategy C, the recovery process was significantly slower even with a very large Hill coefficient (e.g., $m = 10$). For the cases with small Hill coefficients (e.g., $m \leq 4$) that are commonly used in stem cell modeling (17, 32), more than 50 cell cycles were needed to recover the stem cell population to a level near the levels observed in A and B. These results indicate that complex feedback mechanisms incorporating epigenetic states provide faster recovery after sudden damage in stem cell tissues.

We also note that the distributions of the cell epigenetic states show different dynamics for homogeneous or heterogeneous proliferation probabilities. If the proliferation is homogeneous (strategies A and C), the cell distributions remain unchanged during the process. When the proliferation is heterogeneous (strategy B), the cell distribution reshapes after a decrease in cell population and then regains its original form; however, this period is longer than the recovery time of the population (Fig. 3 *B* and *C*).

Next, we induced a temporary increase in the differentiation probability. Physiologically, this type of increase can be induced by a decrease in differentiated cells through a negative feedback mechanism regulating the differentiation process (see refs. 52 and 53 for examples of HSC). We study the three strategies to determine which ones induce a response to effectively replenish the lost cells.

The three strategies yielded different dynamics regarding cell populations. Strategy B provided less variation in the total cell population, a higher level of differentiated cells during the increasing phase of differentiation, and a faster recovery to the normal level after the differentiation probability regained its value (Fig. 4 *A* and *B*). Moreover, for the homogenous proliferating cells, strategy A induced a better response compared with strategy C in terms of smaller variance in the cell population and a higher level of differentiated cells during the increase of the differentiation probability (Fig. 4 *A* and *B*, red and blue lines). These results indicate that an optimal control strategy proposed here with the heterogeneous proliferation probability can lead to good adaptation to temporal changes in the differentiation probability to sustain the cell population and effectively replenish decreases in downstream differentiated cells.

The three strategies also yielded different dynamics for tissue epigenetics $f_t(x)$. For strategies A and C, a clear shift in $f_t(x)$ occurred toward the low-performance region ($x < 60$, see Fig. 2, *Inset* for the performance function) during the increases in

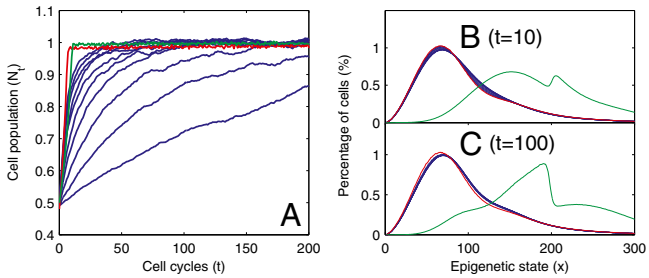

Fig. 3. Recovery of the cell population and distribution of epigenetic states after a sudden loss of half of the total population of cells. (*A*) Cell population time courses. (*B*) The function $f_t(x)$ at $t = 10$ cell cycles after the sudden loss. (*C*) The function $f_t(x)$ at $t = 100$ cell cycles after the sudden loss. Three different controls are shown: strategy A (red), B (greed), and C (blue). For strategy C, the Hill coefficient m varies from 1 to 10 (from bottom to top in *A*). The cell populations at homeostasis are normalized to their maximum levels. See *SI Text*, section S5 for other parameters used in simulations.

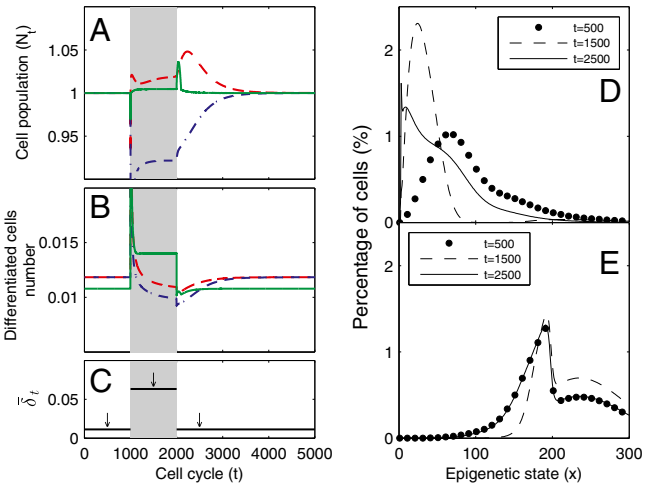

Fig. 4. Tissue response to temporal changes in differentiation. (*A*) Cell population time courses under three different strategies for proliferation. The red dashed line represents strategy A, the green solid line strategy B, and the blue dashed/dotted line strategy C with the Hill coefficient $m = 10$. (*B*) Time course of the number of differentiated cells $(N_t\bar{\delta}_t)$. (*C*) Time course of average differentiation $\bar{\delta}_t$. Shadows indicate the time window of increasing differentiation. (*D*) Cell distributions (strategy A) at three time points (marked with arrows in *C*), before (filled circles, $t = 500$), during (dashed line, $t = 1{,}500$), and after (solid line, $t = 2{,}500$) the temporal change of differentiation. (*E*) Same as *D* but using strategy B.

differentiation, and a slow recovery occurred after the differentiation level returned to its normal level (Fig. 4*D*). For strategy B, the tissue epigenetics shifted to its higher performance region $(x > 100)$ and recovered quickly after the differentiation level returned to normal (Fig. 4*E*). These results suggest that an optimal control strategy using heterogeneous proliferation can lead to a better robust response in the epigenetic states of resting phase stem cells after a sudden increase in differentiation.

In response to the severe loss of hematopoietic cells, dormant HSCs may shift their niches and become injury-activated HSCs (10). We modeled this effect by introducing an increase in the resting phase cell population along with an increase in differentiation probability (*SI Text*, section S3). In comparison with the case in Fig. 4, only a minor difference in the transient dynamics is observed with the similar long-time dynamics between the two cases, and the results regarding the characteristics of the three strategies remain the same.

In addition, we also examined the tissue response to temporal increases in apoptosis, which is often observed in diseases or clinical treatments (e.g., during chemotherapy). The simulations again showed that an optimal control strategy based on heterogeneous proliferation leads to less variation in cell populations (*SI Text*, section S3). The overall results demonstrate the apparent advantages of the control strategy of heterogeneous proliferation in robust responses to perturbations during tissue growth.

Successful Evolution Depends on the Selection of both Epigenetic States and Cell Populations. When mutation occurs, the fitness function W varies with evolutionary time. For simplicity, we only considered mutations affecting the apoptosis $\bar{\mu}_G(x)$ and the proliferation probability $\bar{\beta}_{1,G}$ (see *SI Text*, section S5 for simulation details) and ignore their effects on the differentiation $\bar{\delta}_G(x)$. Assuming mutations of higher fitness are more likely to survive, we investigated the evolution of apoptosis to maximize the evolutionary fitness.

First, we studied the three different strategies (A, B, and C) with the apoptosis probability being initialized as a constant and with low performance at the beginning of the evolution period

(Fig. 2*B*). Following the evolution of apoptosis, all three strategies caused high performance and stable cell populations (Fig. 5 *A–C*). In comparison with the traditional simple feedback (strategy C), the optimal control strategies (A and B) showed faster evolutionary dynamics and less fluctuations in the cell population. During the evolution period, the average cell performance function $\overline{\chi}$ obviously increased, but only a small change in the cell population was observed. The $\overline{\chi}$ dynamics originate from genome mutations that alter the apoptosis $\overline{\mu}_G(x)$, and the performance $\overline{\chi}$ during homeostasis is a consequence of the optimal control of proliferation that depends on the epigenetic states during each cell cycle. Thus, the increasing of $\overline{\chi}$ during evolution indicates that cross-talk occurs between genetic and epigenetic regulation.

An example of the evolution in apoptosis using strategy B is shown in Fig. 6, and this example suggests the tendency to choose a high apoptosis probability for cells with low performance and low apoptosis probability for cells with high performance. Consequently, the tissue epigenetics $f(x)$ during homeostasis shifts from a profile of low-performance cells dominating at the beginning to the profile of high-performance cells dominating at the end during evolution. These results indicate that the evolutionary fitness function W automatically leads to an evolution of effective apoptosis that eliminates low-performance cells and maintains high tissue performances. The evolutionary dynamics using strategy A show similar results, and the resulting apoptosis $\overline{\mu}_G(x)$ is insensitive to its initial probability and the differentiation $\overline{\delta}_G(x)$ (*SI Text*, section S4).

Finally, we investigated whether it is possible to have successful evolution based on a fitness function defined only with epigenetic states or with cell populations. To this end, we replaced the fitness function W with either $\overline{\chi}$ or $\varphi(N)$. When only the epigenetics $\overline{\chi}$ were considered, strategy A and C produced successful evolution of high performance and persistent cell populations (Fig. 5*D*). However, strategy B caused a marked increase in the cell population (Fig. 5*D*, *Inset*) that originated from the proliferation $\overline{\beta}_{1,G}$, which changed at each mutation but was not selected in the evolution process. In contrast, when $\varphi(N)$ was chosen as the evolutionary fitness, all three strategies failed to select an apoptosis probability function to produce high performance due to the absence of cross-talk between the genetic control and the epigenetics regulation. This finding is shown in Fig. 5*E* in which $\overline{\chi}$ remains a small value in the evolutionary process.

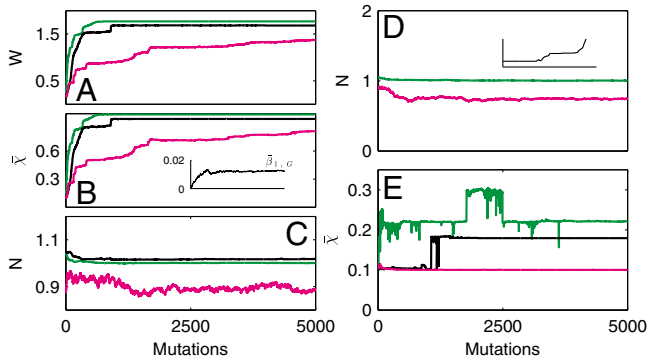

Fig. 5. Evolution dynamics for different control strategies. Time is measured by the number of mutations. Results for strategies A (green), B (black) and C (magenta) are shown using the average of 10 independent sample evolution dynamics. (*A*) Fitness during evolution. (*B*) The cell performance function $\overline{\chi}$. *Inset* shows $\overline{\beta}_{1,G}$ based on strategy B. (*C*) Cell population *N*. (*D*) The cell population when $\overline{\chi}$ is used as the evolutionary fitness. *Inset* shows the dynamics for strategy B in which the population size markedly increases after 1,000 mutations. (*E*) Time course of $\overline{\chi}$ when $\varphi(N)$ is used as the evolutionary fitness.

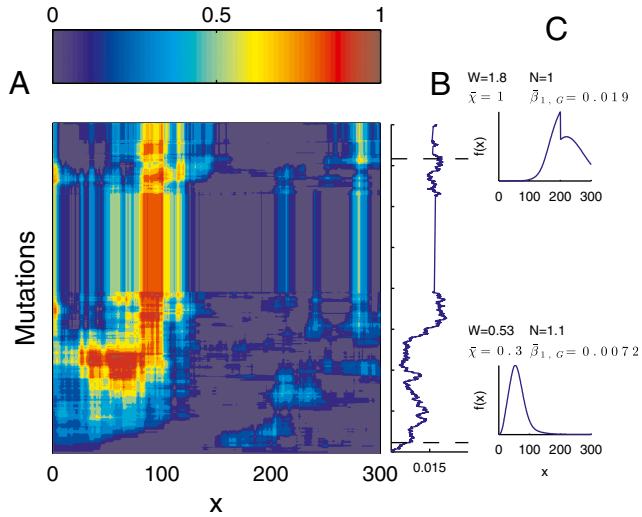

Fig. 6. An example of evolutionary dynamics of the apoptosis $\overline{\mu}_G(x)$ and the proliferation $\overline{\beta}_{1,G}$ following strategy B. (*A*) The evolution of $\overline{\mu}_G(x)$, with the initial $\overline{\mu}_G(x) = 0.07$ for each *x*. (*B*) The proliferation $\overline{\beta}_{1,G}$ that is initiated from $\overline{\beta}_{1,G} = 0$. (*C*) The density $f(x)$ during homeostasis at two time points of mutations, indicated by dashed lines in *B*. Evolutionary fitness *W*, population number *N*, cell performance $\overline{\chi}$, and proliferation probability $\overline{\beta}_{1,G}$ are also given in each case.

Conclusions and Discussion

Adult stem cells in self-renewing tissues are persistent over a long lifespan despite stochastic perturbations and accidental changes. How can stem cells regulate their regeneration during each cell cycle such that the tissue performances (e.g., size of cell populations and cell distributions in epigenetic states) are maintained over the lifetime of tissues? How can stem cells recover robustly after sudden changes? In this paper, we developed a generic modeling framework based on the dynamic programming approach to obtain control strategies that govern the probabilities of proliferation, differentiation, and apoptosis of stem cells. One important feature of the model is its capability of incorporating the performance functions of stem cells at two distinct time scales: the time of one cell cycle and the lifetime of the tissue. Another noteworthy attribute of the model is the representation of stem cells in their epigenetic states to allow cells that are programmed to perform the same functions to exhibit variability and heterogeneity, a characteristic often observed in stem cells.

Using these modeling techniques, we identified controlling strategies that maintain the performance of regeneration tissues (e.g., the desirable distributions of stem cells in their epigenetic states) that are subject to random fluctuations during each cell division. One optimal control inherently emerging from maximizing the performance during each cell cycle is a feedback regulation that controls proliferation through both the cell population and heterogeneous dependence on the epigenetic states. The strategy has an additional advantage compared with the typical feedback regulation that depends only on the size of the cell population, and the advantage entails the speedy recovery of tissue functions after a sudden loss in cells or temporal perturbations in differentiation capability.

While a regenerative tissue needs to reproduce cells in an accurate quantity as well as in a faithful distribution of their epigenetic states within a reasonable time window, the tissue also needs an ability of removing cells that have genetic or epigenetic errors due to mutations or stochastic cellular events. By maximizing the fitness function, our model naturally selects an apoptosis strategy to eliminate the cells with errors. The control strategy

regarding proliferation depends on apoptosis at each cell cycle; therefore, the derived apoptosis regulation demonstrates that cross-talk occurs between epigenetic regulation occurring at a short time scale of one cell cycle and genetic evolution occurring at a long time scale. Recent observations provide strong evidences of how the DNA variant influences the epigenetics (54–56). At the center of the epigenetic-dependent control strategies is the dependence of proliferation on differentiation and apoptosis through a complex feedback mechanism.

The current study is intended to introduce a simple and generic modeling framework without involving any molecular or mechanistic descriptions. To investigate specific functions of one particular type of stem cells, one can add an additional layer of complexity into the model by incorporating corresponding genetic and molecular regulation into the quantities of proliferation, differentiation, and apoptosis. The transition between quiescent and resting phase can also be added to the model for tissues with quiescent stem cells. Additionally, we can study the effect of apoptosis in response to differentiation and proliferation within the same framework, as well as the effect of aging, by introducing a time-dependent performance function. Cell lineages consisting of different cell types along with different performance objectives may also be included in this type of modeling framework. The derived control strategies in this work lack molecular details; however, the qualitative relationships found between the epigenetic states and the three control probabilities can be scrutinized closely using experiments. For example, the three quantities may be estimated using techniques such as fluorescence-activated cell sorting (FACS) if the epigenetic states (e.g., through levels of transcriptional factors) can be marked by fluorescence labels. The distributions of epigenetic states of stem cells at both resting and proliferating phases can be obtained at different times through FACS to estimate the dynamics of the cell population distribution in terms of the epigenetic states. Through these experimental connections, the present work sheds light on how stem cells use proliferation, differentiation, and apoptosis collectively to manage many challenges that regenerative tissues face during each cell cycle and during their lifetime, which may lead to new therapeutic strategies in medical practice. For example, one may control the distribution of stem cell populations using drugs targeting epigenetic components (e.g., special forms of DNA methylation) or alternating the physiological environment so the cells favor particular epigenetic states for better proliferation or better differentiation in an unhealthy tissue.

In this study, the performance function Q, which measures the physiological performance of stem cells, is usually difficult to quantify in real biological tissues because the function is dependent on the complex physiological environment. Nevertheless, it may be possible to estimate the relative performance when two or more types of stem cells compete for a common resource or a niche by which growth factors and other survival signals are provided. The performance of each type of cell depends on the populations as well as the common resource and niches; and therefore, the control strategies for different stem cells affect each other. For this case, the game theoretic approach may be very useful. In general, evolutionary adaptation ensures healthy biological functions and robust response to accidental changes of tissues controlled by stem cells, suggesting that evolution shapes the population biology of stem cells. The methods from population biology and evolutionary theory are helpful in understanding stem cells and their epigenetic regulation.

ACKNOWLEDGMENTS. S.A.L. acknowledges the support of Princeton University's Grand Challenges Program. We thank Terence Hwa and Arthur Lander for stimulating discussions and acknowledge the helpful comments on the manuscript from Marc Mangel, Michael Mackey, and Anastasia Nijnik. This research was supported by the National Natural Science Foundation of China (11272169 and 91229201), and by National Institutes of Health Grants R01GM67247 and P50GM76516, and National Science Foundation Grant DMS1161621.

1. Baylin SB, Jones PA (2011) A decade of exploring the cancer epigenome—biological and translational implications. *Nat Rev Cancer* 11(10):726–734.
2. Sandoval J, Esteller M (2012) Cancer epigenomics: Beyond genomics. *Curr Opin Genet Dev* 22(1):50–55.
3. Huh D, Paulsson J (2011) Non-genetic heterogeneity from stochastic partitioning at cell division. *Nat Genet* 43(2):95–100.
4. Lane SW, Gilliland DG (2010) Leukemia stem cells. *Semin Cancer Biol* 20(2):71–76.
5. Liu S, Dontu G, Wicha MS (2005) Mammary stem cells, self-renewal pathways, and carcinogenesis. *Breast Cancer Res* 7(3):86–95.
6. Vijg J, Suh Y (2013) Genome instability and aging. *Annu Rev Physiol* 75:645–668.
7. Copley MR, Beer PA, Eaves CJ (2012) Hematopoietic stem cell heterogeneity takes center stage. *Cell Stem Cell* 10(6):690–697.
8. Dykstra B, et al. (2007) Long-term propagation of distinct hematopoietic differentiation programs in vivo. *Cell Stem Cell* 1(2):218–229.
9. Ehninger A, Trumpp A (2011) The bone marrow stem cell niche grows up: Mesenchymal stem cells and macrophages move in. *J Exp Med* 208(3):421–428.
10. Trumpp A, Essers M, Wilson A (2010) Awakening dormant haematopoietic stem cells. *Nat Rev Immunol* 10(3):201–209.
11. Lévesque JP, Helwani FM, Winkler IG (2010) The endosteal 'osteoblastic' niche and its role in hematopoietic stem cell homing and mobilization. *Leukemia* 24(12): 1979–1992.
12. Wilson A, Trumpp A (2006) Bone-marrow haematopoietic-stem-cell niches. *Nat Rev Immunol* 6(2):93–106.
13. Wilson A, et al. (2008) Hematopoietic stem cells reversibly switch from dormancy to self-renewal during homeostasis and repair. *Cell* 135(6):1118–1129.
14. Barker N, van de Wetering M, Clevers H (2008) The intestinal stem cell. *Genes Dev* 22 (14):1856–1864.
15. Leedham SJ, Brittan M, McDonald SA, Wright NA (2005) Intestinal stem cells. *J Cell Mol Med* 9(1):11–24.
16. van der Flier LG, Clevers H (2009) Stem cells, self-renewal, and differentiation in the intestinal epithelium. *Annu Rev Physiol* 71:241–260.
17. Lander AD, Gokoffski KK, Wan FY, Nie Q, Calof AL (2009) Cell lineages and the logic of proliferative control. *PLoS Biol* 7(1):e15.
18. Seita J, Rossi DJ, Weissman IL (2010) Differential DNA damage response in stem and progenitor cells. *Cell Stem Cell* 7(2):145–147.
19. Rich T, Allen RL, Wyllie AH (2000) Defying death after DNA damage. *Nature* 407 (6805):777–783.
20. Bondar T, Medzhitov R (2010) p53-mediated hematopoietic stem and progenitor cell competition. *Cell Stem Cell* 6(4):309–322.
21. Marusyk A, Porter CC, Zaberezhnyy V, DeGregori J (2010) Irradiation selects for p53-deficient hematopoietic progenitors. *PLoS Biol* 8(3):e1000324.
22. Wang J, et al. (2012) A differentiation checkpoint limits hematopoietic stem cell self-renewal in response to DNA damage. *Cell* 148(5):1001–1014.
23. Hu GM, Lee CY, Chen YY, Pang NN, Tzeng WJ (2012) Mathematical model of heterogeneous cancer growth with an autocrine signalling pathway. *Cell Prolif* 45(5): 445–455.
24. MacKey MC (2001) Cell kinetic status of haematopoietic stem cells. *Cell Prolif* 34(2): 71–83.
25. Traulsen A, Lenaerts T, Pacheco JM, Dingli D (2013) On the dynamics of neutral mutations in a mathematical model for a homogeneous stem cell population. *J R Soc Interface* 10(79):20120810.
26. Lo WC, et al. (2009) Feedback regulation in multistage cell lineages. *Math Biosci Eng* 6(1):59–82.
27. Mangel M, Bonsall MB (2013) Stem cell biology is population biology: Differentiation of hematopoietic multipotent progenitors to common lymphoid and myeloid progenitors. *Theor Biol Med Model* 10(5):5.
28. Marciniak-Czochra A, Stiehl T, Ho AD, Jäger W, Wagner W (2009) Modeling of asymmetric cell division in hematopoietic stem cells—regulation of self-renewal is essential for efficient repopulation. *Stem Cells Dev* 18(3):377–385.
29. Johnston MD, Edwards CM, Bodmer WF, Maini PK, Chapman SJ (2007) Mathematical modeling of cell population dynamics in the colonic crypt and in colorectal cancer. *Proc Natl Acad Sci USA* 104(10):4008–4013.
30. Mangel M, Bonsall MB (2008) Phenotypic evolutionary models in stem cell biology: Replacement, quiescence, and variability. *PLoS ONE* 3(2):e1591.
31. Dingli D, Traulsen A, Pacheco JM (2007) Stochastic dynamics of hematopoietic tumor stem cells. *Cell Cycle* 6(4):461–466.
32. Rodriguez-Brenes IA, Komarova NL, Wodarz D (2011) Evolutionary dynamics of feedback escape and the development of stem-cell-driven cancers. *Proc Natl Acad Sci USA* 108(47):18983–18988.
33. Chou CS, et al. (2010) Spatial dynamics of multistage cell lineages in tissue stratification. *Biophys J* 99(10):3145–3154.
34. Ovadia J, Nie Q (2013) Stem cell niche structure as an inherent cause of undulating epithelial morphologies. *Biophys J* 104(1):237–246.
35. Burns FJ, Tannock IF (1970) On the existence of a G_0 -phase in the cell cycle. *Cell Tissue Kinet* 3(4):321–334.
36. Mackey MC (1978) Unified hypothesis for the origin of aplastic anemia and periodic hematopoiesis. *Blood* 51(5):941–956.

37. Arrow KJ, Levin SA (2009) Intergenerational resource transfers with random offspring numbers. *Proc Natl Acad Sci USA* 106(33):13702–13706.
38. Mangel M, Ludwig D (1992) Definition and evaluation of the fitness of behavioral and developmental programs. *Annu Rev Ecol Syst* 23:507–536.
39. Nowak MA (2006) *Evolutionary Dynamics: Exploring the Equations of Life* (Belknap Press of Harvard Univ Press, Cambridge, MA).
40. Dodd IB, Micheelsen MA, Sneppen K, Thon G (2007) Theoretical analysis of epigenetic cell memory by nucleosome modification. *Cell* 129(4):813–822.
41. Sennerstam R, Strömberg JO (1986) Cell growth and cell division: Dissociated and random initiated? A study performed on embryonal carcinoma cell lines. II. *Cell Tissue Kinet* 19(1):71–81.
42. Orr HA (2009) Fitness and its role in evolutionary genetics. *Nat Rev Genet* 10(8): 531–539.
43. Bellmann R (1957) *Dynamic Programming* (Princeton Univ Press, Princeton), pp 11, 64, 70.
44. Houston A, McNamara JM (1999) *Models of Adaptive Behaviour* (Cambridge Univ Press, Cambridge, UK).
45. Mangel M, Clark CW (1988) *Dynamic Modeling in Behavioral Ecology* (Princeton Univ Press, Cambridge, UK).
46. Bullough WS (1975) Mitotic control in adult mammalian tissues. *Biol Rev Camb Philos Soc* 50(1):99–127.
47. Challen GA, et al. (2012) Dnmt3a is essential for hematopoietic stem cell differentiation. *Nat Genet* 44(1):23–31.
48. Hu G, et al. (2013) H2A.Z facilitates access of active and repressive complexes to chromatin in embryonic stem cell self-renewal and differentiation. *Cell Stem Cell* 12(2):180–192.
49. Akbarzadeh S, et al. (2002) Tyrosine residues of the granulocyte colony-stimulating factor receptor transmit proliferation and differentiation signals in murine bone marrow cells. *Blood* 99(3):879–887.
50. Pulsipher MA, et al. (2009) Adverse events among 2408 unrelated donors of peripheral blood stem cells: Results of a prospective trial from the National Marrow Donor Program. *Blood* 113(15):3604–3611.
51. Stroncek DF, et al. (1993) Experiences of the first 493 unrelated marrow donors in the National Marrow Donor Program. *Blood* 81(7):1940–1946.
52. Price TH, Chatta GS, Dale DC (1996) Effect of recombinant granulocyte colony-stimulating factor on neutrophil kinetics in normal young and elderly humans. *Blood* 88(1):335–340.
53. Silva M, et al. (1996) Erythropoietin can promote erythroid progenitor survival by repressing apoptosis through Bcl-XL and Bcl-2. *Blood* 88(5):1576–1582.
54. Kasowski M, et al. (2013) Extensive variation in chromatin states across humans. *Science* 342(6159):750–752.
55. Kilpinen H, et al. (2013) Coordinated effects of sequence variation on DNA binding, chromatin structure, and transcription. *Science* 342(6159):744–747.
56. McVicker G, et al. (2013) Identification of genetic variants that affect histone modifications in human cells. *Science* 342(6159):747–749.

Supporting Information

Lei et al. 10.1073/pnas.1324267111

SI Text

S1. Model Description

Intercell Cycle Transformation. Our model describes the dynamics of resting phase stem cell population N_t, and the distribution density of cell epigenetic states $f_t(x)$. Here x is a variable representing the epigenetic state of a cell, and subscript t indicates the tth cell cycle. At each cell cycle, cells undergo proliferation [with a probability $\beta_t(x)$], apoptosis [with a probability $\mu_t(x)$], and differentiation [with a probability $\delta_t(x)$], so that $(N_t, f_t(x))$ changes from one cell cycle to the next:

$$(N_t, f_t(x)) \mapsto (N_{t+1}, f_{t+1}(x)). \qquad \textbf{[S1]}$$

During each cell cycle, $N_t \int f_t(x)\delta_t(x)dx$ cells leave the resting phase due to differentiation, and $N_t \int f_t(x)\beta_t(x)dx$ cells enter the proliferation phase. Each cell in the proliferation phase either goes through apoptosis with a probability $\mu_t(x)$ or produces two daughter cells. Here we omit the transitions between resting and quiescent phase. Hence, the cell population after mitosis is

$$\begin{aligned} N_{t+1} &= N_t - N_t \int f_t(x)\delta_t(x)dx - N_t \int f_t(x)\beta_t(x)dx \\ &\quad + 2N_t \int f_t(x)\beta_t(x)(1-\mu_t(x))dx \\ &= N_t\left(1 + \int f_t(x)[\beta_t(x)(1-2\mu_t(x)) - \delta_t(x)]dx\right). \end{aligned}$$

The integrals are taken over all possible epigenetic states. Define the observed proliferation probability as

$$\beta_{t,\text{obs}} = 1 + \int f_t(x)[\beta_t(x)(1-2\mu_t(x)) - \delta_t(x)]dx, \qquad \textbf{[S2]}$$

then

$$N_{t+1} = N_t \beta_{t,\text{obs}}. \qquad \textbf{[S3]}$$

Here $\beta_{t,\text{obs}}$ is the ratio of cell population numbers between two consecutive cell cycles.

To obtain the transformation of $f_t(x)$, we introduce a transition probability $p(x,y)$, representing the probability that a daughter cell of state x comes from a mother cell of state y. Then

$$\int p(x,y)dx = 1 \qquad \textbf{[S4]}$$

for all y.

Similarly to the above argument, at each cell cycle, the number of cells with state x is $N_t f_t(x)$. After a cell division, $N_t f_t(x)(\delta_t(x) + \beta_t(x))$ cells with state x are removed from the resting phase due to differentiation and proliferation, and $2N_t \int f_t(y)\beta_t(y)(1-\mu_t(y))p(x,y)dy$ cells of state x are produced after mitosis. Thus, after mitosis, the number of cells with state x becomes

$$\begin{aligned} N_{t+1} f_{t+1}(x) &= N_t f_t(x) - N_t f_t(x)(\delta_t(x) + \beta_t(x)) \\ &\quad + 2N_t \int f_t(y)\beta_t(y)(1-\mu_t(y))p(x,y)dy, \end{aligned}$$

which gives

$$\begin{aligned} f_{t+1}(x) = \frac{1}{\beta_{t,\text{obs}}} \Big[& f_t(x)(1-(\delta_t(x)+\beta_t(x))) \\ & + 2\int f_t(y)\beta_t(y)(1-\mu_t(y))p(x,y)dy \Big]. \end{aligned} \qquad \textbf{[S5]}$$

Eqs. **S2**, **S3**, and **S5** together define transformation **S1**.

Evolutionary Fitness Function. To define an evolutionary fitness function akin to natural selection, we first introduce a tissue performance function Q, which depends on the cell population through a function $\varphi(x)$ and the distribution density $f_t(x)$ through a cell performance function $\chi(x)$:

$$Q(N_t, f_t(x)) = \varphi(N_t) \int \chi(x) f_t(x)dx. \qquad \textbf{[S6]}$$

At each cell cycle, $(N_{t+1}, f_{t+1}(x))$ changes according to **[S3]** and **[S5]**, and depends on the quantities $\{\beta_t(x), \gamma_t(x), \delta_t(x)\}$. Thus, given $(N_t, f_t(x))$, we have

$$\begin{aligned} Q(N_{t+1}, f_{t+1}(x)) &= \varphi(N_{t+1}) \int \chi(x) f_{t+1}(x)dx \\ &= \varphi(N_t\beta_{t,\text{obs}}) \int \chi(x) \frac{1}{\beta_{t,\text{obs}}} \Big[f_t(x)\big(1-(\delta_t(x)+\beta_t(x))\big) \\ &\quad + 2f_t(y)\beta_t(y)\big(1-\mu_t(y)\big)p(x,y)dy \Big] dx \\ &= \frac{\varphi(N_t\beta_{t,\text{obs}})}{\beta_{t,\text{obs}}} \Big[\int \chi(x) f_t(x)(1-(\delta_t(x)+\beta_t(x)))dx \\ &\quad + 2\iint \chi(x) f_t(y)\beta_t(y)(1-\mu_t(y))p(x,y)dxdy \Big], \end{aligned}$$

where $\beta_{t,\text{obs}}$ is defined by **[S2]**. Let

$$\begin{aligned} & Q(N_t, f_t(x) | \beta_t(x), \mu_t(x), \delta_t(x)) \\ &= \frac{\varphi(N_t\beta_{t,\text{obs}})}{\beta_{t,\text{obs}}} \Big[\int \chi(x) f_t(x)\Big(1-(\delta_t(x)+\beta_t(x))\Big)dx \\ &\quad + 2\iint \chi(x) f_t(y)\beta_t(y)\big(1-\mu_t(y)\big)p(x,y)dxdy \Big], \end{aligned} \qquad \textbf{[S7]}$$

then

$$Q(N_{t+1}, f_{t+1}(x)) = Q\Big(N_t, f_t(x) | \beta_t(x), \mu_t(x), \delta_t(x)\Big), \qquad \textbf{[S8]}$$

which depends on $\beta_t(x)$, $\mu_t(x)$ and $\delta_t(x)$.

In **[S7]**, the proliferation probability $\beta_t(x)$ varies at each cell cycle by epigenetic regulation; the apoptosis probability $\mu_t(x) = \overline{\mu}_G(x) + \hat{\mu}_t(x)$ in which $\overline{\mu}_G(x)$ is the average probability at homeostasis and is selected through genetic mutations and $\hat{\mu}_t(x)$ is random at each cell cycle due to epigenetic modulations. Similarly, the differentiation probability takes the form $\delta_t(x) = \overline{\delta}_G(x) + \hat{\delta}_t(x)$ in which $\overline{\delta}_G(x)$ is the average probability at homeostasis and $\hat{\delta}_t(x)$ represents the epigenetic uncertainty.

At each cell cycle, the proliferation $\beta_t(x)$ is controlled to achieve maximum tissue performance in Q after one cell division

in the face of uncertainties in apoptosis $\mu_t(x)$ and differentiation $\delta_t(x)$. This leads to solving the corresponding Bellman condition for $Q(N_{t+1}, f_{t+1}(x))$:

$$\mathrm{E}_{\mu_t(x),\delta_t(x)} \max_{\beta_t(x)} Q\Big(N_t, f_t(x) \big| \beta_t(x), \mu_t(x), \delta_t(x)\Big), \qquad \textbf{[S9]}$$

where $\mathrm{E}_{\mu_t(x),\delta_t(x)}$ is the expectation with respect to apoptosis and differentiation probabilities during cell division.

The procedure of solving **[S9]** is given below. At each cell cycle, the expectations of $\mu_t(x)$ and $\delta_t(x)$ are given as

$$\mathrm{E}\mu_t(x) = \mu_{t-1}(x), \qquad \mathrm{E}\delta_t(x) = \delta_{t-1}(x).$$

The proliferation rate $\beta_t(x)$ is obtained by solving the Bellman condition:

$$\begin{aligned}
&\max_{\beta_t(x)} \mathrm{E}Q\Big(N_t, f_t(x) \big| \beta_t(x), \mu_t(x), \delta_t(x)\Big) \\
&\approx \max_{\beta_t(x)} \frac{\varphi(N_t \mathrm{E}\beta_{t,\mathrm{obs}})}{\mathrm{E}\beta_{t,\mathrm{obs}}} \Bigg[\int \chi(x) f_t(x) \Big(1 - \big(\delta_{t-1}(x) + \beta_t(x)\big)\Big) dx \\
&\quad + 2 \iint \chi(x) f_t(y) \beta_t(y) \big(1 - \mu_{t-1}(y)\big) p(x,y) dx dy \Bigg],
\end{aligned}$$

where $\mathrm{E}\beta_{t,\mathrm{obs}}$ is the expectation of the observed proliferation probability

$$\begin{aligned}
\mathrm{E}\beta_{t,\mathrm{obs}} &= 1 + \int f_t(x) \Big[\beta_t(x)\big(1 - 2\mathrm{E}\mu_t(x)\big) - \mathrm{E}\delta_t(x)\Big] dx \\
&= 1 + \int f_t(x) \Big[\beta_t(x)\big(1 - 2\mu_{t-1}(x)\big) - \delta_{t-1}(x)\Big] dx.
\end{aligned}$$

After $\beta_t(x)$ is solved by the Bellman condition, stochastic perturbations for $\mu_t(x)$ and $\delta_t(x)$ are introduced, resulting in

$$\mu_t(x) = \overline{\mu}_G(x) + \hat{\mu}_t(x), \qquad \delta_t(x) = \overline{\delta}_G(x) + \hat{\delta}_t(x). \qquad \textbf{[S10]}$$

Hence, the observed proliferation probability becomes

$$\beta_{t,\mathrm{obs}} = 1 + \int f_t(x) \Big[\beta_t(x)\big(1 - 2\mu_t(x)\big) - \delta_t(x)\Big] dx \qquad \textbf{[S11]}$$

with $\mu_t(x)$ and $\delta_t(x)$ given by **[S10]**. Consequently, the tissue state $(N_{t+1}, f_{t+1}(x))$ becomes

$$N_{t+1} = N_t \beta_{t,\mathrm{obs}} \qquad \textbf{[S12]}$$

$$\begin{aligned}
f_{t+1}(x) = \frac{1}{\beta_{t,\mathrm{obs}}} \Bigg[& f_t(x) \Big(1 - \big(\delta_t(x) + \beta_t(x)\big)\Big) \\
& + 2 \int f_t(y) \beta_t(y) \big(1 - \mu_t(y)\big) p(x,y) dy \Bigg].
\end{aligned} \qquad \textbf{[S13]}$$

Given $(\overline{\mu}_G(x), \overline{\delta}_G(x))$ that are selected through genetic mutations in long time, **[S12]** and **[S13]** define a lifespan dynamics of $(N_t, f_t(x))$.

The evolutionary fitness function is defined as the performance at homeostasis after many cell divisions (i.e., $t \to \infty$):

$$W = \lim_{t \to \infty} Q\big(N_t, f_t(x)\big). \qquad \textbf{[S14]}$$

The fitness W is dependent on the probabilities $\overline{\mu}_G(x)$ and $\overline{\delta}_G(x)$ that are selected through genetic mutations.

S2. Homeostasis State

Nonlinear Integral Equations. During the development and maturation of an organism, $(N_t, f_t(x))$ evolves following **[S3]** and **[S5]**. At homeostasis, $(N_t, f_t(x))$ approaches an equilibrium state, which is represented as the limit as $t \to \infty$ (it may be more accurate to be referred to as the average of the limits when there are stochastic fluctuations).

Let $(N, f(x), \beta(x), \overline{\mu}_G(x), \overline{\delta}_G(x))$ be averages of the limits $(N_t, f_t(x), \beta_t(x), \mu_t(x), \delta_t(x))$ when $t \to \infty$. At homeostasis, the stem cell population reaches equilibrium and therefore $\beta_{t,\mathrm{obs}} \to 1$ as $t \to \infty$, which yields

$$\int f(x) \Big[\beta(x)\big(1 - 2\overline{\mu}_G(x)\big) - \overline{\delta}_G(x)\Big] dx = 0. \qquad \textbf{[S15]}$$

Furthermore, from **[S5]** the homeostasis tissue epigenetics $f(x)$ satisfies integral equation

$$\begin{aligned}
f(x) = & f(x)\big(1 - \big(\overline{\delta}_G(x) + \beta(x)\big)\big) \\
& + 2 \int f(y) \beta(y) (1 - \overline{\mu}_G(y)) p(x,y) dy,
\end{aligned} \qquad \textbf{[S16]}$$

or equivalently,

$$f(x) = \frac{2 \int f(y) \beta(y) \big(1 - \overline{\mu}_G(y)\big) p(x,y) dy}{\overline{\delta}_G(x) + \beta(x)}, \qquad \textbf{[S17]}$$

with a normalization condition

$$\int f(x) dx = 1. \qquad \textbf{[S18]}$$

Thus, for given functions $\overline{\mu}_G(x)$, $\overline{\delta}_G(x)$, and $p(x,y)$, the proliferation $\beta(x)$ and distribution density $f(x)$ are given by nonnegative solutions of the nonlinear integral Eqs. **S15**, **S17**, and **S18**.

The mathematical questions related to the existence and uniqueness of nonnegative solutions of **[S15]**, **[S17]**, and **[S18]** are left for future study. Here, we only investigate a simple case for illustration.

Heterogeneous Apoptosis Can Improve the Maintenance of Tissue Epigenetics. We assume all cells are homogeneous in proliferation so that $\beta(x)$ is independent of x. Consequently, **[S15]** gives

$$\beta = \frac{\int f(x) \overline{\delta}_G(x) dx}{\int f(x) \big(1 - 2\overline{\mu}_G(x)\big) dx}, \qquad \textbf{[S19]}$$

and **[S17]** can be rewritten as a nonlinear integral equation

$$f(x) = \frac{2 \iint f(y) f(z) \overline{\delta}_G(z) \big(1 - \overline{\mu}_G(y)\big) p(x,y) dy dz}{\int f(y) \Big(\overline{\delta}_G(x) \big(1 - 2\overline{\mu}_G(y)\big) + \overline{\delta}_G(y)\Big) dy}. \qquad \textbf{[S20]}$$

Next we show that *if* $\overline{\mu}_G(x)$ is independent of x, the tissue epigenetics at homeostasis is abnormal. We consider a specific situation in which each cell only takes one of the two discrete epigenetic states, with $x \in \Omega_1$ implying a defective cell and $x \in \Omega_2$ a normal cell. The functions $\overline{\delta}_G(x)$ and $p(x,y)$ are given by piecewise constant functions:

$$\overline{\delta}_G(x) = \begin{cases} \delta_1, & x \in \Omega_1 \\ \delta_2, & x \in \Omega_2, \end{cases}$$

and

$$p(x,y)=\begin{cases} p_1(x), & y\in\Omega_1 \\ p_2(x), & y\in\Omega_2, \end{cases}$$

and let

$$p_{i,j}=\int_{x\in\Omega_i} p_j(x)dx, \quad (i,j=1,2). \qquad \textbf{[S21]}$$

Furthermore, we make the following assumptions to induce normal differentiated cells and reduce defective cells number:

1. Defective cells have smaller differentiation probabilities than normal cells ($\delta_1\le\delta_2$).
2. The transition rate from defective to normal cells is smaller than that of the reverse transition ($p_{2,1}\le p_{1,2}$).

Denoting

$$f_1=\int_{y\in\Omega_1} f(y)dy, \quad f_2=\int_{y\in\Omega_2} f(y)dy, \qquad \textbf{[S22]}$$

and taking $x\in\Omega_1$, **[S20]** becomes [we note $\overline{\mu}_G(y)=\mu$ being a constant]

$$f(x)=\frac{2(f_1\delta_1+f_2\delta_2)(1-\mu)\left(f_1p_1(x)+f_2p_2(x)\right)}{\delta_1(1-2\mu)+f_1\delta_1+f_2\delta_2}. \qquad \textbf{[S23]}$$

Integrating **[S23]** over $x\in\Omega_1$, we obtain

$$f_1=\frac{2(f_1\delta_1+f_2\delta_2)(1-\mu)\left(f_1p_{1,1}+f_2p_{1,2}\right)}{\delta_1(1-2\mu)+f_1\delta_1+f_2\delta_2}. \qquad \textbf{[S24]}$$

Since $f_2=1-f_1$, **[S24]** is an equation of f_1 in the form

$$F_1(f_1)=F_2(f_1), \qquad \textbf{[S25]}$$

where

$$F_1(f_1)=f_1\left(\delta_1(1-2\mu)+\delta_2-(\delta_2-\delta_1)f_1\right),$$

$$F_2(f_1)=2(1-\mu)\left(\delta_2-(\delta_2-\delta_1)f_1\right)\left(f_1\left(p_{1,1}-p_{1,2}\right)+p_{1,2}\right).$$

We note that both $F_1(f_1)$ and $F_2(f_1)$ are quadratic functions of f_1. There are two roots of $F_1(f_1)=0$ $\left(0 \text{ and } \frac{(1-2\mu)\delta_1+\delta_2}{\delta_2-\delta_1}\right)$, and two roots of $F_2(f_1)=0\left(-\frac{p_{12}}{p_{11}-p_{12}}(<0) \text{ and } \frac{\delta_2}{\delta_2-\delta_1}\left(<\frac{(1-2\mu)\delta_1+\delta_2}{\delta_2-\delta_1}\right)\right)$. Then the equation $F_1(f_1)=F_2(f_1)$ has a unique solution f_1^* in the interval $\left(0,\frac{\delta_2}{\delta_2-\delta_1}\right)$ (Fig. S1). Here f_1^* gives the percentage of defective cells. Furthermore, if $F_1(z)\le F_2(z)$ then $f_1^*\ge z$ (see Fig. S1 for an illustration).

Now, from the above two assumptions,

$$\begin{aligned} F_1\left(\frac{1}{2}\right)&=\frac{1}{2}\left((1-2\mu)\delta_1+\frac{1}{2}(\delta_1+\delta_2)\right)\\ &=\frac{1}{2}(1-\mu)(\delta_1+\delta_2)-\frac{1}{2}\left(\delta_2+\mu(\delta_2-\delta_1)\right)\\ &\le\frac{1}{2}(1-\mu)(\delta_1+\delta_2), \end{aligned}$$

and

$$\begin{aligned} F_2\left(\frac{1}{2}\right)&=\frac{1}{2}(1-\mu)(\delta_1+\delta_2)(p_{11}+p_{12})\\ &\ge\frac{1}{2}(1-\mu)(\delta_1+\delta_2)(p_{11}+p_{21})\\ &=\frac{1}{2}(1-\mu)(\delta_1+\delta_2). \end{aligned}$$

Thus, $F_1\left(\frac{1}{2}\right)<F_2\left(\frac{1}{2}\right)$ and hence $f_1^*\ge\frac{1}{2}$. This result indicates that more than half of the cells are defective at homeostasis, an abnormal or a disease state for a tissue.

S3. Optimal Control Strategies

The Problem of Variation. At each cell cycle, the proliferation probability $\beta_t(x)$ is determined by Bellman condition **S9**. From **[S9]**, the function $\beta_t(x)$ is taken so that the expectation of $Q(N_{t+1},f_{t+1}(x))$ reaches the maximum, with $(N_{t+1},f_{t+1}(x))$ given by $(N_t,f_t(x))$ through **[S2]**, **[S3]**, and **[S5]**.

First, we show that Bellman condition **S9** alone is not sufficient to determine the function $\beta_t(x)$, and thus additional restrictions are required for a well-posed problem.

We assume that in the tissue $\mu_t(x)$ and $\delta_t(x)$ are known before the proliferation $\beta_t(x)$ is chosen. Define a functional

$$A[\beta_t]=Q(N_{t+1},f_{t+1}(x))=\varphi(N_{t+1})\int\chi(x)f_{t+1}(x)dx. \qquad \textbf{[S26]}$$

Here N_{t+1} and $f_{t+1}(x)$ depend on β_t through **[S2]**, **[S3]**, and **[S5]**. If $A[\beta_t]$ attains its local minimum at β_0 and $\eta(x)$ is an arbitrary function,

$$A[\beta_0]\le A\left[\beta_0+\varepsilon\eta\right] \qquad \textbf{[S27]}$$

for any small number ε. Therefore, the variation of A at $\beta_t=\beta_0$ must vanish,

$$\begin{aligned} \left.\frac{dA[\beta_0+\varepsilon\eta]}{d\varepsilon}\right|_{\varepsilon=0}&=\left[\varphi'(N_{t+1})\int\chi(x)f_{t+1}(x)dx\frac{dN_{t+1}}{d\varepsilon}\right.\\ &\left.+\varphi(N_{t+1})\frac{d\int\chi(x)f_{t+1}(x)dx}{d\varepsilon}\right]\Bigg|_{\varepsilon=0}=0. \end{aligned} \qquad \textbf{[S28]}$$

A direct calculation yields

$$\left.\frac{dN_{t+1}}{d\varepsilon}\right|_{\varepsilon=0}=N_t\int\eta(x)f_t(x)(1-2\mu_t(x))dx$$

and

$$\begin{aligned} &\left.\frac{d\int\chi(x)f_{t+1}(x)dx}{d\varepsilon}\right|_{\varepsilon=0}\\ &=\frac{1}{\beta_{t,\text{obs}}}f_{t+1}(x)\left(\int\eta(x)f_t(x)\left(1-2\mu_t(x)\right)dx\right)\\ &+\frac{1}{\beta_{t,\text{obs}}}\\ &\times\left(-\eta(x)f_t(x)+2\int\eta(y)f_t(y)(1-\mu_t(y))p(x,y)dy\right). \end{aligned}$$

Here $\beta_{t,\text{obs}}$ and $f_{t+1}(x)$ are given by **[S2]** and **[S5]**, respectively, but with $\beta_t = \beta_0$. Thus, Eq. **S28** yields, for an arbitrary function $\eta(x)$,

$$\begin{aligned} 0 &= \varphi'(N_{t+1})N_{t+1} \\ &\times \left(\int \chi(x) f_{t+1}(x)dx\right)\left(\int \eta(x) f_t(x)\left(1-2\mu_t(x)\right)dx\right) \\ &+ 2\varphi(N_{t+1})\int \eta(y) f_t(y)\left(1-\mu_t(y)\right)p(x,y)dy \\ &+ \varphi(N_{t+1}) f_{t+1}(x)\int \eta(y) f_t(y)\left(1-2\mu_t(y)\right)dy \\ &- \varphi(N_{t+1})\eta(x) f_t(x). \end{aligned} \qquad \textbf{[S29]}$$

It is impossible to find a function $\beta_0(x)$ that solves **[S29]** with arbitrary x and function $\eta(x)$.

The above argument shows that Bellman condition **S9** does not have a solution for a general function $\beta_t(x)$, and thus additional conditions are required.

For a particular biological system, there are additional restrictions to the proliferation. We consider two types of stem cells often seen in biological systems, namely either homogeneous or heterogeneous in their proliferation. For stem cells homogenous in their proliferation, the function $\beta_t(x)$ is independent of x (but may change with t); for stem cells heterogeneous in proliferation, the function $\beta_t(x)$ varies with x.

Homogeneous in Proliferation (Strategy A). ***Formulation of the proliferation probability.*** For cells homogeneous in their proliferation, the proliferation probability β_t is independent of the epigenetic state x. It is implicitly assumed that cells know the expected apoptosis probability $\mu_t(x)$ and the differentiation probability $\delta_t(x)$ before determining the proliferation probability β_t. For example, a simple strategy is to assume the expectations of these two probabilities equal the current values while determining β_t, i.e., assuming $\mathrm{E}\mu_t(x) = \mu_{t-1}(x)$ and $\mathrm{E}\delta_t(x) = \delta_{t-1}(x)$.

Since β_t is a constant, the optimal value is given by $\partial Q(N_{t+1}, f_{t+1}(x))/\partial\beta_t = 0$, which yields

$$\begin{aligned} 0 &= \varphi'(N_{t+1})\frac{\partial N_{t+1}}{\partial \beta_t}\int \chi(x) f_{t+1}(x) \\ &+ \varphi(N_{t+1})\int \chi(x)\frac{\partial f_{t+1}(x)}{\partial \beta_t}dx. \end{aligned} \qquad \textbf{[S30]}$$

Let

$$\bar{\mu}_t = \int f_t(x)\mu_t(x)dx, \quad \bar{\delta}_t = \int f_t(x)\delta_t(x)dx,$$

$$\bar{\chi}_t = \int f_t(x)\chi(x)dx, \quad \bar{d}_t = \int f_t(x)\chi(x)\delta_t(x)dx,$$

$$\sigma(y) = \int \chi(x)p(x,y)dx, \quad \bar{\sigma}_t = \frac{\int f_t(y)(1-\mu_t(y))\sigma(y)dy}{1-\bar{\mu}_t},$$

then we have

$$\frac{\partial N_{t+1}}{\partial \beta_t} = N_t(1-2\bar{\mu}_t),$$

$$\begin{aligned} \frac{\partial f_{t+1}(x)}{\partial \beta_t} &= -\frac{f_{t+1}(x)}{N_{t+1}}\frac{\partial N_{t+1}}{\partial \beta_t} + \frac{N_t}{N_{t+1}} \\ &\times \left[-f_t(x) + 2\int f_t(y)(1-\mu_t(y))p(x,y)dy\right]. \end{aligned}$$

Thus, **[S30]** becomes

$$\frac{N_t\beta_{t,\text{obs}}\varphi'\left(N_t\beta_{t,\text{obs}}\right)}{\varphi\left(N_t\beta_{t,\text{obs}}\right)} = A_t, \qquad \textbf{[S31]}$$

where

$$A_t = 1 - \frac{\bar{\sigma}_t}{\bar{\chi}_{t+1}} - \frac{\bar{\sigma}_t - \bar{\chi}_t}{(1-2\bar{\mu}_t)\bar{\chi}_{t+1}},$$

$$\bar{\chi}_{t+1} = \frac{\bar{\chi}_t - \bar{d}_t + \beta_t(2(1-\bar{\mu}_t)\bar{\sigma}_t - \bar{\chi}_t)}{\beta_{t,\text{obs}}}$$

and

$$\beta_{t,\text{obs}} = 1 + \beta_t(1-2\bar{\mu}_t) - \bar{\delta}_t. \qquad \textbf{[S32]}$$

The theoretical optimal strategy β_t is obtained from a solution of **[S31]** and **[S32]**. In addition, we note a biologically acceptable proliferation probability is always nonnegative, and must be less than a maximum value $\beta_{\max}$ that is limited by its biological capability. Thus, the possible proliferation probability takes values within the interval $[0, \beta_{\max}]$. We set the probability $\beta_t = 0$ if the β_t obtained above is less than 0, and set $\beta_t = \beta_{\max}$ if it is larger than $\beta_{\max}$.

Assume the population performance $\varphi(N)$ is maximum at $N = N_*$, i.e., $\varphi'(N_*) = 0$ and $\varphi''(N_*) < 0$. Here N_* is by definition the fittest cell population of the tissue. In **[S31]**, if A_t is close to 0, we have approximately

$$\beta_{t,\text{obs}} \approx \frac{1}{N_*}\left(N_* + \frac{A_t\varphi(N_*)}{N_*\varphi''(N_*)}\right), \qquad \textbf{[S33]}$$

or equivalently,

$$\beta_t \approx \frac{\frac{1}{N_t}\left(N_* + \frac{A_t\varphi(N_*)}{N_*\varphi''(N_*)}\right) - 1 + \bar{\delta}_t}{1-2\bar{\mu}_t}. \qquad \textbf{[S34]}$$

Therefore,

$$N_{t+1} \approx N_* + \frac{A_t\varphi(N_*)}{N_*\varphi''(N_*)}, \qquad \textbf{[S35]}$$

which yields $N_t \approx N_*$ when A_t is close to 0. Thus, **[S34]** indicates a negative feedback when the cell population is close to the value of the fittest population (Fig. S2*A*).

Tissue dynamics based on strategy A. Fig. S2 shows numerical simulations obtained from the above control strategy. Fig. S2*A* plots the decreasing dependence of proliferation probability on cell population. Fig. S2*B* shows the time course of the performance $Q(N_t, f_t(x))$ in a simulation of 5,000 cell cycles. Fig. S2*C* gives $f_t(x)$ at the early, intermediate, and later temporal points in the simulation.

Epigenetic dependences are required for robust development and evolution. In this study, the dependences of δ, μ, χ on the epigenetic state are significant in regulation. Here we study the importance of epigenetic dependence in robust development and evolution.

From **[S3]** and **[S5]**, the dynamics of population and average cell performance $(N_t, \bar{\chi}_t)$ are given by

$$\begin{bmatrix} N_t \\ \bar{\chi}_t \end{bmatrix} \mapsto \begin{bmatrix} N_t\beta_{t,\text{obs}} \\ \dfrac{\bar{\chi}_t - \bar{d}_t + \beta_t(2(1-\bar{\mu}_t)\sigma_t - \bar{\chi}_t)}{\beta_{t,\text{obs}}} \end{bmatrix} \qquad \textbf{[S36]}$$

Here

$$\beta_t = \frac{\beta_{t,\mathrm{obs}} - 1 + \bar{\delta}_t}{1 - 2\bar{\mu}_t}. \quad \textbf{[S37]}$$

Eqs. **S5**, **S31**, **S36**, and **S37** together define a dynamical system for $(N_t, \bar{\chi}_t)$. This dynamical system reaches a statistical equilibrium state when $t \to \infty$. Thus, the expectation $\mathrm{E}\beta_{t,\mathrm{obs}} \to 1$ and the limits

$$N = \lim_{t\to\infty} \mathrm{E}N_t, \quad \bar{\chi} = \lim_{t\to\infty} \mathrm{E}\bar{\chi}_t$$

are well defined. In this case, we have

$$\frac{N\varphi'(N)}{\varphi(N)} = \lim_{t\to\infty} \mathrm{E}A_t \quad \textbf{[S38]}$$

and

$$\bar{\chi} = \lim_{t\to\infty} \mathrm{E}\left[\bar{\sigma}_t + (1 - 2\bar{\mu}_t)\left(\bar{\sigma}_t - d_t/\bar{\delta}_t\right)\right]. \quad \textbf{[S39]}$$

Eqs. **S38** and **S39** give the population N and average performance $\bar{\chi}$ at homeostasis.

If the performance function χ is independent of the state x (i.e., $\bar{\chi}_t = \bar{\sigma}_t = \chi$ for any t), we have $N = N_*$ and therefore the evolutionary fitness $W = \bar{\chi}\varphi(N_*)$ is independent of the apoptosis probability $\mu(x)$. Hence, the apoptosis response fails to evolve based on the evolutionary fitness W. This result suggests that variability in cell performance is necessary for successful natural selection for apoptosis.

When the cell fitness $\chi(x)$ varies with x, [**S35**] indicates $N \neq N_*$, i.e., the cell population at homeostasis differs from the value of the fittest population, and the difference $\Delta N = |N - N_*|$ is proportional to $\Delta\chi = |\sigma - \chi|$. We note that $\Delta\chi$ measures the difference between the performance of mother cells and their daughter cells, and is in turn determined by $p(x,y)$—the variation between daughter cells and the mother cell due to epigenetic state transition in cell division. Simulations show that if the daughter cells are identical to their mother cells, i.e.,

$$p(x,y) = \begin{cases} 1 & x = y \\ 0 & x \neq y, \end{cases} \quad \textbf{[S40]}$$

then $N = N_*$, and the tissue epigenetics $f(x)$ at homeostasis is dependent on the initial cell distributions (Fig. S3). We note that changes in cell distributions during a lifetime can be induced by accidental injury. Thus, the above analysis suggest that the transition of epigenetic state in cell division is necessary for a robust tissue epigenetics at homeostasis with respect to accidental changes in life span, but can shift the stem cell population away from the value of the fittest population.

Heterogeneous in Proliferation (Strategy B). ***Formulation of the proliferation probability.*** For stem cells heterogeneous in proliferation, $\beta_t(x)$ varies with the epigenetic state x. Here we study a simple situation in which cells take two distinct proliferation probabilities.

We divide all stem cells into two phenotypes by their epigenetic state x, with $x \in \Omega_1$ for type I cells, and $x \in \Omega_2$ for type II cells. Proliferation probabilities are the same for cells of the same type:

$$\beta_t(x) = \begin{cases} \beta_{t,1}, & x \in \Omega_1 \\ \beta_{t,2}, & x \in \Omega_2 \end{cases}. \quad \textbf{[S41]}$$

We assume that the proliferation of type II cells is modulated such that $\beta_{t,2}$ changes at each cell cycle, while the proliferation of type I cells is unmodulated over the lifetime ($\beta_{t,1} \equiv \bar{\beta}_{1,G}$ is genetically regulated).

Based on the above assumptions, the proliferation $\beta_{t,2}$, for given $\beta_{t,1} \equiv \bar{\beta}_{1,G}$, $\mu_t(x)$ and $\delta_t(x)$, is determined by $\partial Q(N_{t+1}, f_{t+1}(x))/\partial\beta_{t,2} = 0$, i.e.,

$$\bar{\chi}_{t+1}\varphi'(N_{t+1})\frac{\partial N_{t+1}}{\partial\beta_{t,2}} + \varphi(N_{t+1})\frac{\partial\bar{\chi}_{t+1}}{\partial\beta_{t,2}} = 0, \quad \textbf{[S42]}$$

which gives

$$N_{t+1}\frac{\varphi'(N_{t+1})}{\varphi(N_{t+1})} = 1 - \frac{2\int_{\Omega_2} f_t(y)(1-\mu_t(y))\sigma_t(y)dy - \int_{\Omega_2} f_t(x)\chi(x)dx}{\bar{\chi}_{t+1}\int_{\Omega_2} f_t(x)(1-2\mu_t(x))dx}, \quad \textbf{[S43]}$$

with $N_{t+1} = N_t\beta_{t,\mathrm{obs}}$.

At each cell cycle, the optimal proliferation probability $\beta_{t,2}$ is obtained based on Eq. **S43**.

To solve Eq. **S43**, we denote

$$\bar{f}_{t,1} = \int_{\Omega_1} f_t(x)dx, \quad \bar{f}_{t,2} = \int_{\Omega_2} f_t(x)dx,$$

$$\bar{\mu}_{t,1} = \int_{\Omega_1} f_t(x)\mu_t(x)dx, \quad \bar{\mu}_{t,2} = \int_{\Omega_2} f_t(x)\mu_t(x)dx,$$

$$\bar{\chi}_{t,1} = \int_{\Omega_1} f_t(x)\chi(x)dx, \quad \bar{\sigma}_{t,1} = \frac{\int_{\Omega_1} f_t(x)(1-\mu_t(x))\sigma(x)dx}{f_{t,1} - \bar{\mu}_{t,1}},$$

$$\bar{\chi}_{t,2} = \int_{\Omega_2} f_t(x)\chi(x)dx, \quad \bar{\sigma}_{t,2} = \frac{\int_{\Omega_2} f_t(x)(1-\mu_t(x))\sigma(x)dx}{f_{t,2} - \bar{\mu}_{t,2}}.$$

Then,

$$\beta_{t,\mathrm{obs}} = 1 + \bar{\beta}_{1,G}\left(\bar{f}_{t,1} - 2\bar{\mu}_{t,1}\right) + \beta_{t,2}\left(\bar{f}_{t,2} - 2\bar{\mu}_{t,2}\right) - \bar{\delta}_t, \quad \textbf{[S44]}$$

and

$$\begin{aligned}
\bar{\chi}_{t+1} &= \frac{1}{\beta_{t,\mathrm{obs}}}\int \chi(x)f_t(x)(1-\delta_t(x)-\beta_t(x))dx \\
&\quad + \frac{2}{\beta_{t,\mathrm{obs}}}\int f(y)\beta_t(y)(1-\mu_t(y))\sigma(y)dy \\
&= \frac{1}{\beta_{t,\mathrm{obs}}}\Big[\left(\bar{\chi}_t - \bar{d}\right)_t - \bar{\beta}_{1,G}\bar{\chi}_{t,1} - \beta_{t,2}\bar{\chi}_{t,2} \\
&\quad + 2\bar{\beta}_{1,G}\left(\bar{f}_{t,1} - \bar{\mu}_{t,1}\right)\bar{\sigma}_{t,1} + 2\beta_{t,2}\left(\bar{f}_{t,2} - \bar{\mu}_{t,2}\right)\bar{\sigma}_{t,2}\Big] \\
&= \frac{1}{\beta_{t,\mathrm{obs}}}\Big[\left(\bar{\chi}_t - \bar{d}\right)_t - \bar{\beta}_{1,G}\left(\bar{\chi}_{t,1} - 2\left(\bar{f}_{t,1} - \bar{\mu}_{t,1}\right)\bar{\sigma}_{t,1}\right) \\
&\quad - \beta_{t,2}\left(\bar{\chi}_{t,2} - 2\left(\bar{f}_{t,2} - \bar{\mu}_{t,2}\right)\bar{\sigma}_{t,2}\right)\Big].
\end{aligned} \quad \textbf{[S45]}$$

Thus, we can rewrite [**S43**] as

$$N_t\beta_{t,\mathrm{obs}}\frac{\varphi'\left(N_t\beta_{t,\mathrm{obs}}\right)}{\varphi\left(N_t\beta_{t,\mathrm{obs}}\right)}=A_t' \qquad \textbf{[S46]}$$

with

$$A_t'=1-\frac{\overline{\sigma}_{t,2}}{\overline{\chi}_{t+1}}-\frac{f_{t,2}\overline{\sigma}_{t,2}-\overline{\chi}_{t,2}}{\overline{\chi}_{t+1}\left(f_{t,2}-2\overline{\mu}_{t,2}\right)}. \qquad \textbf{[S47]}$$

The proliferation $\beta_{t,2}$ is obtained from the positive solution of Eqs. **S44–S47**.

Similarly to the previous argument, when $N_t\approx N_*$ and $A_t'\approx 0$, we have

$$\beta_{t,\mathrm{obs}}\approx\frac{1}{N_*}\left(N_*+\frac{A_t'\varphi(N_*)}{N_*\varphi''(N_*)}\right), \qquad \textbf{[S48]}$$

and hence

$$\beta_{t,2}\approx\frac{\frac{1}{N_t}\left(N_*+\frac{A_t'\varphi(N_*)}{N_*\varphi''(N_*)}\right)-1-\overline{\beta}_{1,G}\left(\overline{f}_{t,1}-2\overline{\mu}_{t,1}\right)+\overline{\delta}_t}{\overline{f}_{t,2}-2\overline{\mu}_{t,2}}. \qquad \textbf{[S49]}$$

Tissue dynamics based on strategy B. Based on the previous arguments, the proliferation probability of type II cells at homeostasis, denoted as β_2, is dependent on the probability of type I cells $\overline{\beta}_{1,G}$. Fig. S4*A* shows the dependences of β_2 and the evolutionary fitness W on $\overline{\beta}_{1,G}$ (varying from 0 to 0.1). Simulations suggest that the proper value of the unmodulated proliferation probability $\overline{\beta}_{1,G}$ can improve the evolutionary fitness compared with the case of homogeneous proliferation (the corresponding evolutionary fitness is shown by the red dashed line in Fig. S4*A*). We also note that if $\overline{\beta}_{1,G}$ is too large ($\overline{\beta}_{1,G}>0.08$ in the current simulation), it is possible to induce uncontrolled growth such that the fitness decreases to 0. Fig. S4*B* shows tissue epigenetics $f(x)$ at homeostasis with $\overline{\beta}_{1,G}=0.02$ and $\overline{\beta}_{1,G}=0.06$, respectively. When $\overline{\beta}_{1,G}=0.02$, the tissue epigenetics has the same profile as in the case of homogenous proliferation (Fig. S2*C*), and when $\overline{\beta}_{1,G}=0.06$ (with better fitness), the epigenetic distribution shows apparent shift to the region of better performance (corresponding to the region of larger x).

Robust recovery after sudden changes. Fig. S5 shows tissue response (cell population, differentiated cell population, and cell distributions) to temporal changes in differentiation. In simulations, the immigration of dormant cells from the quiescent phase to the resting phase is taken into account in a simple way by introducing a sudden increase (10%) of the resting phase cell population at the time point ($t=1,000$) along with an increase in the differentiation probability. We observe a transient rise and fall of cell populations in the resting phase due to the addition of resting-phase cells to the model, however, with similar long-time dynamics shown in Fig. 4. The overall features are found to be similar to those obtained without considering the effect of the quiescent phase.

Fig. S6 shows cell population dynamics, under three different strategies, when there are temporary changes in the apoptosis probability. The results indicate that heterogeneity in proliferation induces less changes in cell populations than the cases of homogeneous proliferation.

S4. Evolution

The evolutionary fitness W defined by **[S14]** is a function of $\overline{\mu}_G(x)$ and $\overline{\delta}_G(x)$. Here we keep $\overline{\delta}_G(x)$ unchanged and study the evolution of the apoptosis probability $\overline{\mu}_G(x)$ via the fitness function W.

Fig. S7 shows a numerical simulation for the evolution of $\overline{\mu}_G(x)$ when the cells are homogeneous in proliferation. In the simulation, the apoptosis $\overline{\mu}_G(x)$ starts from a constant function ($\overline{\mu}_G(x)\equiv 0.07$) with a low fitness ($W=0.18$), and automatically evolves to yield a high fitness ($W=1.8$) at the end of the simulation. The resulting apoptosis is taken such that cells with lower performance (cells with $x<60$) have larger apoptosis probability. Consequently, the tissue epigenetics $f(x)$ at homeostasis shifts from the profile of low-performance cells being dominant to that of high-performance cells being dominant (Fig. S7*B*). Furthermore, simulations show that the evolution obviously increases the average cell fitness ($\overline{\chi}$ increases from 0.10 to 0.98 in the simulation), but only results in small changes in the cell population N. Further simulations show that the results are robust and insensitive to the choices of initial apoptosis probability (Fig. S8).

We also test our results using different functions for the differentiation $\overline{\delta}_G(x)$ (Fig. S9). Simulations suggest that different differentiation probabilities can give the same value of evolutionary fitness after a number of mutations, and the resulting apoptosis probability and tissue epigenetics at homeostasis are insensitive to $\overline{\delta}_G(x)$.

S5. Details for Numerical Simulations

Parameter Values and Choices of Functions in the Model. In simulating the model, we need to specify the five functions $p(x,y)$, $\overline{\mu}_G(x)$, $\overline{\delta}_G(x)$, $\chi(x)$, and $\varphi(N)$.

For simplicity, we assume the epigenetic state can be represented as a scalar variable $x\in[0,X_{\max}]$. For example, x can be the expression level of one gene, or the number of nucleosome modifications of a DNA region. In general, x represents an intrinsic cellular state that may change after each cell division. Without loss of generality, the four functions $\chi(x)$, $\overline{\delta}_G(x)$, $\overline{\mu}_G(x)$, and $p(x,y)$ are chosen in a consistent way, as seen in Fig. S10. In particular, because x can be transformed into different values by shifting and reflecting its values, without loss of generality, the region of small values of x corresponds to the low value of the performance function $\chi(x)$. Together, we assume the following characteristics of the five functions:

i) A cell has low performance (low capability of accomplishing its physiological function) when $x<60$, and it has high performance when $100<x<X_{\max}=300$.
ii) Cells defined in the region of $100<x<140$ at resting phase have larger differentiation probability ($\overline{\delta}_G(x)$) than the other cells.
iii) Cells with $80<x<160$ at the proliferative phase have smaller apoptosis probability ($\overline{\mu}_G(x)$), as they have larger differentiation probability.
iv) The transition probability $p(x,y)$ is taken in a form such that only local changes in the epigenetic state are allowed in each cell division.
v) Function $\varphi(N)$ is concave with a maximum value at $N=1$ since we normalize the fittest population to $N_*=1$.

All simulation codes are written in MATLAB (MathWorks) (available upon request). Those functions, as plotted in Fig. S10, then take the following forms in MATLAB:

$$\chi(x)=0.1+0.9\times\mathrm{gamcdf}(x,40,2),$$

$$\overline{\delta}_G(x)=0.01+0.4\times\mathrm{normpdf}(x,120,20),$$

$$\overline{\mu}_G(x)=0.35-27\times\mathrm{normpdf}(x,120,40),$$

$$\varphi(N)=(cN)^2e^{-(cN-1)^2},\quad c=\left(\sqrt{5}+1\right)\Big/2,$$

and for $(x,y)\in[0,300]\times[0,300]$

$$p(x,y)=\begin{cases}\dfrac{1}{C(y)}\psi\left(\dfrac{x}{y}-1;\dfrac{\sqrt{2}}{2},10\right) & \left|\dfrac{x}{y}-1\right|<\dfrac{\sqrt{2}}{2}\\ 0 & \text{otherwise}\end{cases}$$

where

$$\psi(z;a,s)=\left(a^2-z^2\right)^s, C(y)=\int_0^{300}\psi\left(\frac{x}{y}-1;\frac{\sqrt{2}}{2},10\right)dx.$$

Here the functions gamcdf and normpdf are taken for the convenience of programming. The values of 0.9, 0.4, and 27 in $\chi(x)$, $\overline{\delta}_G(x)$ and $\overline{\mu}_G(x)$ can be changed to adjust the difference between the maximum and minimum of these functions. We take the initial population $N_0=0.8$ and the initial distribution density $f_0(x)=1/300$.

For the simple feedback (strategy C), a standard Hill function is used for the feedback function:

$$\beta_t=\beta_0\frac{1+\rho(N_t/K)^m}{1+(N_t/K)^m}, \qquad \textbf{[S50]}$$

in which $\beta_0=0.25$, $\rho=0.05$, $K=0.2$, and m varies from 1 to 10.

Proliferation at Each Cell Cycle. At each step, N_t and $f_t(x)$ are known. We first solve **[S31]** (or **[S46]** for cells heterogeneous in proliferation) for β_t [let $\mu_t(x)=\mu_{t-1}(x)$ and $\delta_t(x)=\delta_{t-1}(x)$ while solving these equations]. Next, we apply random perturbations to the average probabilities $\overline{\mu}_G(x)$ and $\overline{\delta}_G(x)$ to obtain $\mu_t(x)$ and $\delta_t(x)$ at the current step:

$$\mu_t(x)=\overline{\mu}_G(x)+0.08\eta_{t,1}+0.04\xi_{t,1}(x),$$

and

$$\delta_t(x)=\overline{\delta}_G(x)+0.006\eta_{t,2}+0.0008\xi_{t,2}(x).$$

Here $\eta_{t,i}$ represent the external noise to the whole population and are independent random values uniformly distributed in $[-1,\ 1]$ and $\xi_{t,i}(x)$ represent the intrinsic noise to each individual cell and are independent uniform distribution random values in $[-1,\ 1]$ for each value of x. The observed proliferations $\beta_{t,\text{obs}}$ is calculated from the calculated β_t, $\mu_t(x)$ and $\delta_t(x)$. Finally, N_{t+1} and $f_{t+1}(x)$ are obtained from **[S3]** and **[S5]**. The procedure is repeated for 5×10^4 steps until the stationary state is reached. Then calculation of the evolutionary fitness W is carried out.

In mimicking the cells heterogeneous in proliferation, we take $\Omega_1=(200,300]$ and therefore $\Omega_2=[0,200]$. At each cell cycle, after obtaining $\beta_{t,2}$ from **[S46]**, the proliferation probability is given as

$$\beta_t(x)=\overline{\beta}_{1,G}+\left(\beta_{t,2}-\overline{\beta}_{1,G}\right)\frac{1}{1+(x/200)^{100}} \qquad \textbf{[S51]}$$

to smooth out $\beta_t(x)$ at $x=200$.

Evolution of the Apoptosis. To study the evolution of apoptosis probability $\overline{\mu}_G(x)$ akin to natural selection, we start from an initial $\overline{\mu}_G(x)$, and apply a small change to generate a new function μ_{new}. We ask whether the change increases the fitness W. If it does increase the fitness, then it survives, and otherwise, it only survives with a probability $\exp[(W_{\text{new}}-W_{\text{old}})/T]$ with a constant T. In simulations, $\overline{\delta}_G(x)$ remains unchanged. The simulation procedure is given below:

1. Start from an initial function $\overline{\mu}_G(x)$.
2. Calculate the evolutionary fitness $W_{\text{old}}=W(\overline{\mu}_G(x))$ following the above procedure.
3. Perform a mutation [perturb the function $\overline{\mu}_G(x)$ at a randomly selected x] to obtain a new function $\overline{\mu}_{G,\text{new}}(x)$ (for heterogeneous cells, we perturb β_1 as well), and calculate the corresponding evolutionary fitness $W_{\text{new}}=W(\overline{\mu}_{G,\text{new}})$.
4. Accept the new function with a probability $\exp[(W_{\text{new}}-W_{\text{old}})/T]$ ($T=0.01$ in simulations) and let $W=W_{\text{new}}$, $\overline{\mu}_G(x)=\overline{\mu}_{G,\text{new}}(x)$.
5. Go to step 3 or stop the simulation.

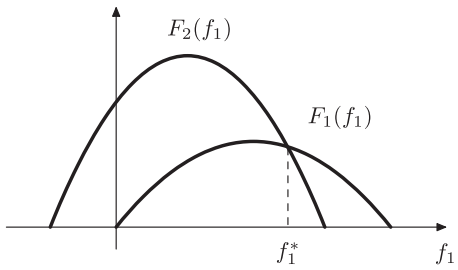

Fig. S1. Illustration of functions $F_1(f_1)$ and $F_2(f_1)$.

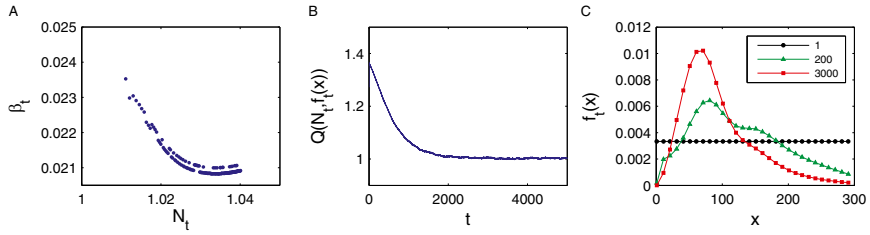

Fig. S2. Simulations for stem cells homogeneous in proliferation. (*A*) Dependence of the proliferation β_t on the size of cell population N_t. (*B*) Time course of the performance $Q(N_t,f_t(x))$. (*C*) Tissue epigenetic $f(x)$ at the cell cycle $t=1$ (black circles), 200 (green triangles), and 3,000 (red squares). See the main text and *SI Text*, section S5 for details.

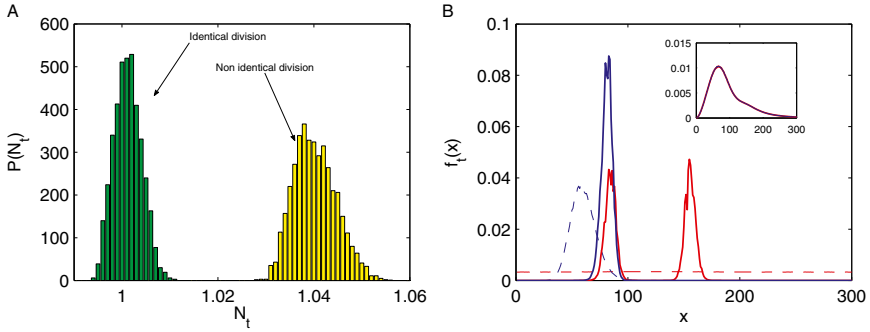

Fig. S3. Simulations with different partition functions $p(x,y)$. (*A*) Distributions of cell populations at homeostasis for identical cell division ($p(x,y)$ given by [**S40**]) and nonidentical cell division [$p(x,y)$ as in Fig. S2], respectively. (*B*) Distributions of epigenetic states obtained from identical cell division but with different initial states (shown by dashed curves of the same color). *Inset* shows distributions obtained from nonidentical cell division but with different initial distributions (the two resulting curves are indistinguishable).

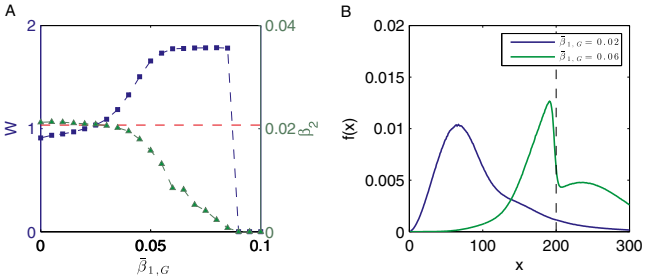

Fig. S4. Numerical simulations for heterogenous stem cells. (*A*) The fitness (*W*, left-hand ordinate and blue squares) as well as proliferation probability of type II cells (β_2, right-hand ordinate and green triangles) at homeostasis as functions of proliferation probability of type I cells $\bar{\beta}_{1,G}$. The red dashed line shows the evolutionary fitness *W* at homeostasis when we assume homogeneous proliferation (strategy A). (*B*) Tissue epigenetics $f(x)$ at homeostasis with $\bar{\beta}_{1,G}=0.02$ (blue) and $\bar{\beta}_{1,G}=0.06$ (green), respectively. The dashed vertical line indicates the separation of type I and II cells. In simulations, all functions are the same as those used in Fig. S2, type I cells are those with $200<x\leq 300$, and type II cells are those with $0\leq x\leq 200$.

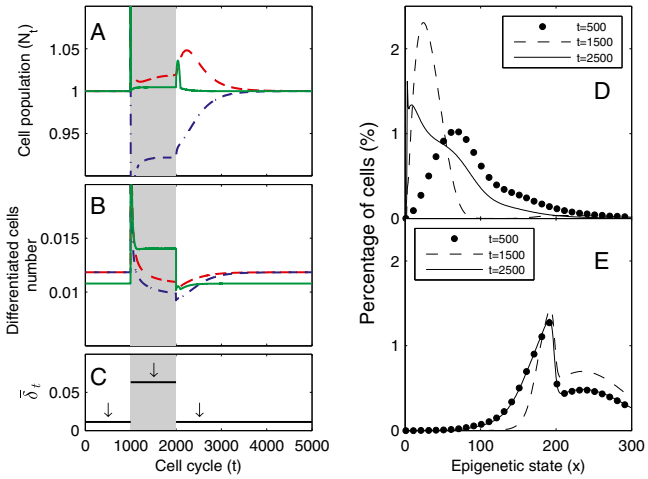

Fig. S5. Tissue response to temporal changes in differentiation. (*A*) Time courses of cell population, under three different strategies for the proliferation. The red dashed line represents strategy A, the green solid line strategy B, and the blue dashed/dotted line strategy C with Hill coefficient $m = 10$. (*B*) Time course of the number of differentiated stem cell $(N_t\bar{\delta}_t)$. (*C*) Time course of the average differential $\bar{\delta}_t$. Shadows indicate the time window of increasing differentiation. (*D*) Cell distributions (strategy A) at three time points (marked with arrows in *C*), before (filled circles, $t = 500$), during (dashed line, $t = 1{,}500$), and after (solid line, $t = 2{,}500$) the sudden change of differentiation. (*E*) Same as *D* but using strategy B.

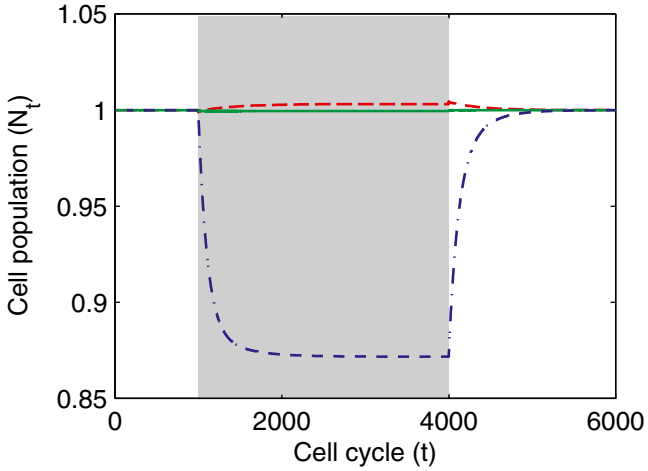

Fig. S6. Simulation of cell population dynamics when there are temporary changes in the apoptosis probability. Different colored lines correspond to different control strategies for proliferation. The red dashed line represents strategy A, the green solid line strategy B, and the blue dashed/dotted line strategy C. The shadow region indicates the time window of increasing the apoptosis probability [$\bar{\mu}_G(x) = 0.35 - 22 \times \mathrm{normpdf}(x, 120, 40)$ in the shadow region].

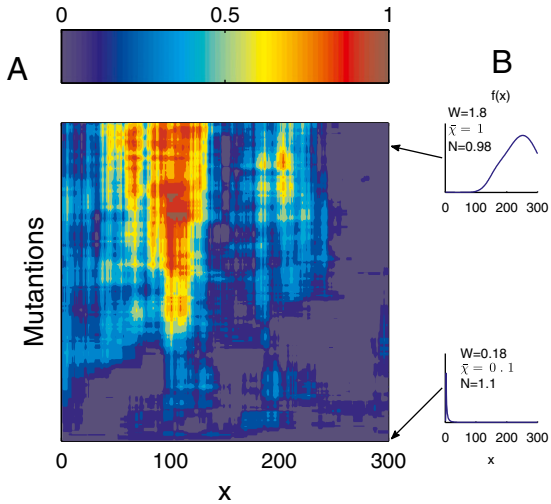

Fig. S7. Evolution of apoptosis probability $\bar{\mu}_G(x)$ of homogenous cells. (*A*) The function $\bar{\mu}_G(x)$ at different times, with an initial constant function $\bar{\mu}_G(x) = 0.07$. (*B*) Tissue genetics $f(x)$, evolutionary fitness *W*, average cell fitness $\bar{\chi}$, and population number *N* at two temporal points (indicated by arrows, early and later in the evolution, respectively). See *SI Text*, section S5 for simulation details.

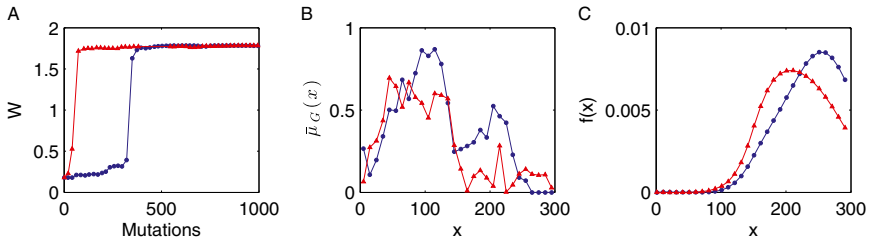

Fig. S8. Evolution of the apoptosis probability starting from different initial functions. (*A*) Dependence of the evolutionary fitness *W* on the number of mutations. (*B*) Apoptosis probability function at the end of the simulation. (*C*) Tissue epigenetics $f(x)$ at the end of simulation. Blue circles are obtained from the initial $\bar{\mu}_G(x) = 0.07$, and red triangles from the initial $\bar{\mu}_G(x) = 0.01 + 0.03 \times \text{chi2pdf}(x,200)$.

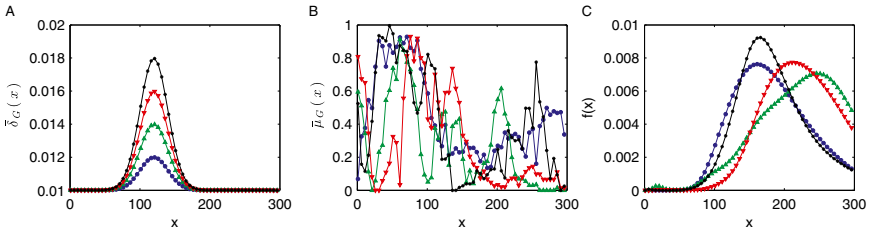

Fig. S9. Evolution of the apoptosis probability $\bar{\mu}_G(x)$ with different forms of $\bar{\delta}_G(x)$. (*A*) The function $\bar{\delta}_G(x)$ used in simulations. We take $\bar{\delta}_G(x) = 0.01 + r \times \text{normpdf}(x,120,20)$ with $r = 0.1$ (blue circles), 0.2 (green up triangles), 0.3 (red down triangles), and 0.4 (black asterisks). (*B*) Apoptosis probability at the end of simulation. (*C*) Tissue epigenetics $f(x)$ at the end of simulation.

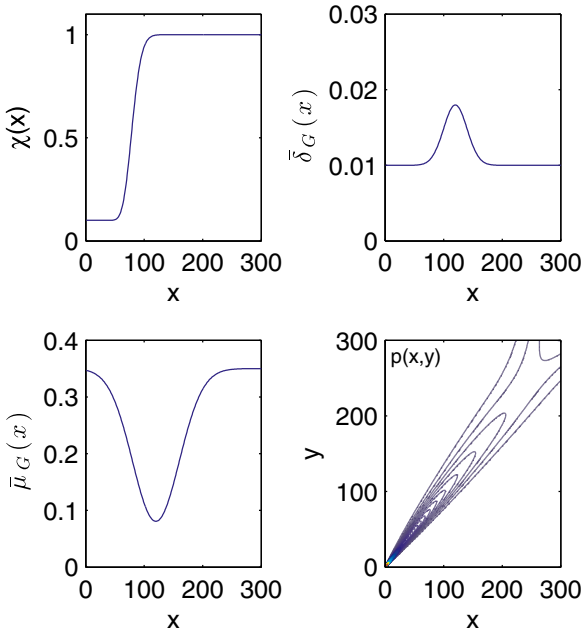

Fig. S10. The functions $\chi(x)$, $\bar{\delta}_G(x)$, $\bar{\gamma}_G(x)$, and $p(x,y)$ (contour plot) used in the simulations.